Review Article
Molecular imaging probe development: a chemistry perspective

Donald D Nolting[1,*], Michael L Nickels[1,*], Ning Guo[1], Wellington Pham[1,2,3]

[1]Vanderbilt University Institute of Imaging Science; [2]Department of Biomedical Engineering, Vanderbilt University; [3]Vanderbilt Ingram Cancer Center; *These authors contributed equally to this work.

Abstract: Molecular imaging is an attractive modality that has been widely employed in many aspects of biomedical research; especially those aimed at the early detection of diseases such as cancer, inflammation and neurodegenerative disorders. The field emerged in response to a new research paradigm in healthcare that seeks to integrate detection capabilities for the prediction and prevention of diseases. This approach made a distinct impact in biomedical research as it enabled researchers to leverage the capabilities of molecular imaging probes to visualize a targeted molecular event non-invasively, repeatedly and continuously in a living system. In addition, since such probes are inherently compact, robust, and amenable to high-throughput production, these probes could potentially facilitate screening of preclinical drug discovery, therapeutic assessment and validation of disease biomarkers. They could also be useful in drug discovery and safety evaluations. In this review, major trends in the chemical synthesis and development of positron emission tomography (PET), optical and magnetic resonance imaging (MRI) probes are discussed.

Keywords: Positron emission tomography, radiochemistry, MRI, optical probes, molecular imaging

Introduction

Molecular imaging is an attractive modality that has been widely employed in many aspects of biomedical research; especially those aimed at the early detection of diseases such as cancer [1], inflammation [2] and neurodegenerative disorders [3]. The field emerged in response to a new research paradigm in healthcare that seeks to integrate detection capabilities for the prediction and prevention of diseases. This approach made a distinct impact in biomedical research as it enabled researchers to leverage the capabilities of molecular imaging probes to visualize a targeted molecular event non-invasively, repeatedly and continuously in a living system. In addition, since such probes are inherently compact, robust, and amenable to high-throughput production, these probes could potentially facilitate screening of preclinical drug discovery, therapeutic assessment and validation of disease biomarkers. They could also be useful in drug discovery and safety

evaluations.

An important precursor to molecular imaging is that it requires multidisciplinary input from other areas including biology, biophysics, bioengineering, molecular biology, chemistry and the clinical sciences [4]. Nevertheless, chemistry has been an inseparable aspect of molecular imaging from the earliest days of its development. In fact, it appears to be the rate-limiting step in the translational development of this emerging science.

In the past decade, the number of scientific reports on the chemical development of molecular imaging probes has increased remarkably [5], there presently are only a few systematic reviews of the chemical synthesis of imaging probes available [6-10]. Moreover, none are presented in a cross-discipline context. In this article, we will address major trends in the chemical synthesis and development of positron emission tomography (PET), optical and

magnetic resonance imaging (MRI) probes.

Chemistry of nuclear imaging probes

Introduction to PET

PET is a non-invasive, *in vivo* imaging technique that uses relatively short-lived positron-emitting radioisotopes (**Figure 1**) either in their pure form or as part of a larger molecule designed and synthesized with the isotope either incorporated within or appended onto the structure. The phenomenon of emitting a positron, which is defined as the antimatter particle to an electron, allows the unstable isotope to shed some of its unnecessary positive charge transforming the atom into a more stable atomic form. Once a positron has been emitted, it will travel a small distance, dictated by the amount of energy the particle was emitted with, from its origin and then encounter an electron, which are plentiful in comparison to the number of positrons. Once this occurs, the two particles will come together and destroy each other in an event termed annihilation. This process converts the total mass of both the positron and electron to pure energy in the form of two 511 keV photons of light traveling 180 degrees away from each other. Detection of these photons is traditionally accomplished by placing the subject into a ring of detectors that have been programmed to differentiate between actual positron decay, i.e. two photons striking detectors on opposite sides of the ring, and background radiation that may be coming from a variety of sources.

In an effort to probe the physiological processes occurring within an organism, radioisotope-containing drugs are injected into the organism of interest and then given time to localize in the areas for which it was designed to target. Once localization has sufficiently occurred, the amount of radiation within the targeted type of tissue or the tissue containing a greater amount of the molecular species of interest will be much larger than the surrounding tissue; this is referred to as contrast. One major physiological process that has received a good deal of attention is that of disease. Since molecular imaging with PET is sensitive to and informative towards the disease processes, researchers have the ability to gain an in-depth understanding of how diseases progress [11]. In addition to imaging biochemical pathways associated with diseases, PET has been widely used in both basic research and clinical settings for imaging tissue pharmacokinetics, tumor response, cell proliferation, gene expression and the status of receptors or tumors along with the diagnoses of heart disease, epilepsy, and stroke [12, 13].

Fluorine-18 labeling methodologies

Fluorine-18 (^{18}F) is an attractive positron-emitter for three main reasons; first, ^{18}F possesses a longer half-life compared to other tracers used in clinical PET studies, second, ^{18}F decay emits a positron of relatively low energy providing a low maximum distance travelled in tissue (2.4 mm) before an annihilation event, and third, steric similarity to a hydrogen atom makes ^{18}F an ideal isotope which can potentially convert any active therapeutic agent into a PET probe without severely hindering the affinity for the molecular target [14, 15].

Formation of ^{18}F-containing molecules can be divided into two main reaction classifications: the first is the formation of an aliphatic or sp^3 hybridized carbon bonded to fluorine and the

Isotope	Halflife (min)	Positron Energy (MeV)	Positron Range (mm)	Production Source
^{82}Rb	1.26	3.15	1.7	generator
^{15}O	2.03	1.70	1.5	cyclotron
^{13}N	9.97	1.19	1.4	cyclotron
^{11}C	20.3	0.96	1.1	cyclotron
^{18}F	109.8	0.64	1.0	cyclotron
^{64}Cu	768	0.66	n/a	cyclotron
^{68}Ga	67.72	1.90	2.9	generator

Figure 1. Commonly used PET radionuclides, their half-lives, range, positron energy, and how they are produced.

second is an aromatic or non-sp^3 hybridized carbon bonded to fluorine. Within these two distinct classes of reaction products, one can consider a wide range of precursors that would enable the formation of the desired fluorinated compounds. In terms of the aliphatic sub-class, which will be discussed first, the type of reaction that fluoride actually undertakes is referred to as a nucleophilic substitution or an S$_N$2 reaction. This type of reaction, as with all reactions, relies on both the reaction conditions and on the presence of a functional group that has a strong ability to be displaced by the weakly nucleophilic fluoride ion.

In order to truly understand the types of reactions that are possible and the steps necessary for obtaining highly reproducible reaction outcomes, one must first understand how and in what form the ^{18}F is obtained. Production of ^{18}F, along with many other positron emitting radionuclides, is accomplished within a cyclotron, which is an instrument that uses alternating magnetic fields that enable the acceleration of either protons or deuterons in a circular fashion. The accelerated particles are eventually directed at a stationary target containing molecular species, such as ^{18}O enriched water (natural isotopic abundance of 0.1%), which is used in the production of the ^{18}F anion [16].

The nuclear reaction that is occurring in this process is [^{18}O(p,n)^{18}F], meaning that the ^{18}O atom absorbs one proton (p) and produces a single ^{18}F atom. During this process one neutron (n) is released. After the production occurs, the fluoride is delivered into a lead shielded box and handled in a way that is intended to protect the chemist from being exposed to high levels of radioactivity. A separate method of producing positron-emitting isotopes is via the use of a generator, which consists of a long-lived isotope that slowly decays into the desired isotope. The most common example of this is a gallium-68 (half-life of 68 minutes) generator, which relies on the decay of germanium-68 (half-life of 271 days) to the desired gallium-68 in the form of gallium(III). This alternative approach will be discussed in a subsequent section.

Once bombardment of the ^{18}O enriched water has been completed, the water now contains a mixture of the desired ^{18}F anion and various other impurities generated during the bombardment of the target. In an effort to recover the valuable ^{18}O enriched water and remove any impurities, the ^{18}F in aqueous solution (H$_2$O/^{18}F$^-$) is passed through an anion-exchange solid phase trapping cartridge allowing the water to pass through and be collected for recycling while trapping the ^{18}F anion. The ^{18}F anion can then be released from the cartridge using either a carbonate or bicarbonate solution containing an appropriate counterion for the ^{18}F anion, such as potassium. Currently, the most popular approach for ^{18}F radiosynthesis is to add a large counter ion, such as tetra-butylammonium salts or the alternative approach of employing Kryptofix [2.2.2] (K$_{222}$) as a chelator of potassium, which has been found to drastically enhance the fluoride reactivity [17]. This act of sequestering the fluoride ion away from the positively charged cations has sometimes been referred to as producing a "naked fluoride ion".

Methods used for enhancing fluoride reactivity rely on variables such as the identity of the solvent used, identity of the fluoride counterion, reaction temperature and the type of heating. The solvent is probably the most commonly manipulated aspect of a fluorination, often determining the success or failure of the reaction. It is well known that polar aprotic solvents and phase transfer catalysts are critical for enhancing the rate of substitution for this type of reaction [18]. The solvent effect of displacement in the second position of pyridine was examined with a variety of nitro precursors in the presence of [^{18}F]KF-K$_{222}$. The reaction yields were high when sulfolane and DMSO were employed as solvents compared to DMF and acetonitrile. However, since sulfolane is a solid at room temperature, DMSO should be an ideal candidate. It is important to note that the reaction will be deactivated in the presence of water. Therefore, it is important to azeotropically remove water from the mixture of kryptofix/[^{18}F]fluoride (from cyclotron) by repeated additions and evaporations of acetonitrile from the reaction vessel before introducing the precursor, which is pre-dissolved in the desired anhydrous solvent. As a challenge to the dogma that polar aprotic solvents are the only solvents capable of enhancing the rate of substitution, it was shown in breakthrough studies that hindered tertiary alcohols will not only promote the fluorination substitution, but greater radiochemical yields (RCYs), which is a measure of the percentage of radioactivity incorporated into the product versus the starting amount of radioactivity, can be
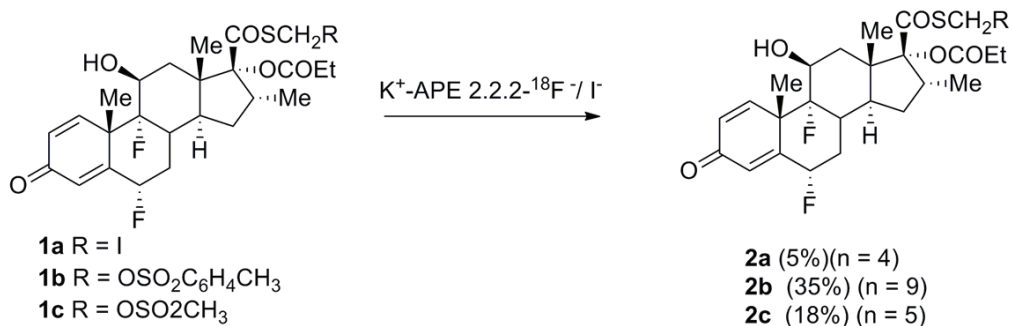
Figure 2. Fluorine-18 labeling of an aliphatic carbon to test the specificity of different leaving groups.

obtained by using the alcohols over the traditional solvents [19, 20].

In terms of heating approaches, both conventional heating and microwave-induced reactions have been used in the radiosynthesis of PET tracers. In recent years, using microwave energy to heat and drive radiochemical reactions has become increasingly popular, especially in the ^{18}F labeling of PET tracers. Microwave-based heating techniques are proving to be valuable tools for speeding up the most commonly occurring reactions in PET radiochemistry, due to both the rapid increase in the temperature of the reaction media and the subsequent shortening of reaction times [21]. Variations on all these reaction parameters can be seen throughout the subsequent sections. Given that changing solvent, temperature and fluoride counterion are generally easy to change from reaction to reaction; the next sections will focus on the choice of the precursors for ^{18}F labeling.
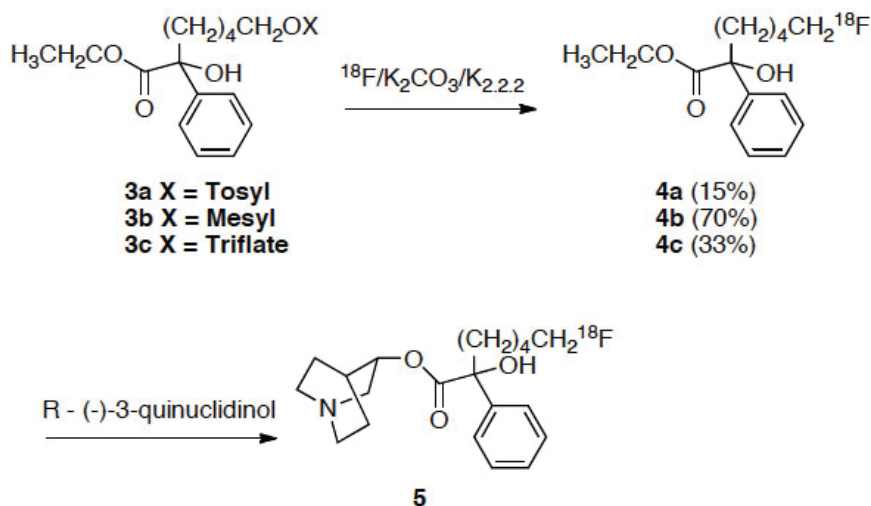
Sulfonic esters

Most PET isotopes have short half-lives and in the case of [^{18}F]fluoride, a weak nucleophilicity. Therefore, labeling processes require careful selection of stable leaving groups that can tolerate the harsh reaction conditions required to obtain a usable level of fluorine reactivity. Designing compounds that not only have the correct reactivity profile, but also, allow a minimum number of steps after the radiolabeling event, presents a challenging problem for chemists and radiochemists alike. Currently, there is no accepted rule of thumb that allows one to determine if a leaving group will produce the desired stability and radiolabeling efficiency. Instead, a complete survey of all reasonable leaving groups is usually necessary to find a species that possesses the correct characteristics.

A successful ^{18}F labeling experiment can be defined by the ability to obtain both high reproducibility and high RCYs, both of which rely on the choice of an appropriately active leaving group for the fluoride anion to displace. In the case of producing an ^{18}F label on an aliphatic carbon, sulfonic esters, such as methane sulphonate (mesylate), trifluoromethylsulphonate (triflate), and *para*-toluenesulphonate (tosylate), are preferred to their halide counterparts. An example of this preference was observed during the development of [S-fluoromethyl-^{18}F] fluticasone propionate 2, a radiotracer developed for lung deposition studies (**Figure 2**). If labeling conditions are held constant and the identity of the leaving group is altered from a halide, such as iodine, to a sulfonic ester, such as a tosylate or mesylate, the reaction proceeds with better RCYs for the sulfonic esters versus their halide counterparts [22]. It is worth noting that the labeling reaction had to be carried out under extremely anhydrous conditions in an effort to avoid inadvertent hydroxide displacement of the leaving group.

The choice of the leaving group, however, varies between chemical targets. Although the reaction rate of displacement using triflate is the best among the sulfonate family, it is generally unstable, which makes this class of compounds difficult to handle, therefore producing low RCYs [23]. This principle was demonstrated during the design and subsequent radiolabeling of 1-azabicyclo[2.2.2]oct-3-yl α,α-(diphenyl)-a-hydroxyacetate (QNB) analog 5 (**Figure 3**) for the imaging of the muscarinic acetylcholinergic receptor (mAChR) [24]. The radiolabeling of 4 was

276

Figure 3. Formation of [18F]-QNB by displacement of various sulfonic esters.

carried out by utilizing different leaving groups such as tosyl, mesyl and triflyl under identical conditions with RCYs of 15, 70 and 33% respectively (decay corrected), clearly showing that the rate of solvolysis of the leaving groups does not always correspond to the percentage of product obtained. Furthermore, this work demonstrates a perfect example of the flexibility in preparing a PET probe; the labeling with the short-lived isotope is not always required to be the last step. As shown in **Figure 3**, the labeled product had to undergo a transesterification step with the sodium salt of 3-quinuclidinol to afford [18F]-QNB **5**. An additional examples are available in the enclosed reference that compare not only the identity of the leaving groups, but also the efficiency of those leaving groups as a function of temperature [22].

Another example to demonstrate the feasibility to incorporate complicated experimental manuveurs during [18F] labeling includes the purification of the radioactive products via distillation. Dimethylthiourea is a scavenger of hydrogen peroxide present in tissue exposed to oxidative stress [25]. The *in vivo* detection of free radicals can be considered an important tool with regard to their role in aging or diseases such as Parkinson's, Alzheimer's, and multiple sclerosis [26]. Due to the additional chemical manipulation, the overall decay corrected RCY for the preparation of N-(2-[18F]fluoroethyl)-N'-methylthiourea (FEMTU) was a modest 25% due to the early introduction of the [18F] source. The overall synthetic yield, however, provided sufficient

amounts of desired product for animal studies. Additional example of this multiple synthesis approach is the development of the myocardial imaging agent (S)-[18F]F-ICI, through the intermediate formation of 1-[18F] fluoro-2-(tosyloxy) ethane which is further reacted with the desired phenol to afford the final product [27, 28]. This was found to be a desired approach over formation of a tosylated product precursor that could be directly reacted with [18F]fluoride to give the product, to the large amount of non-radioactive byproducts formed during the reaction. Employing the fluorinated intermediate gave a much cleaner reaction with greater RCY and a larger amount of radioactivity per mass of product, which is termed specific activity.
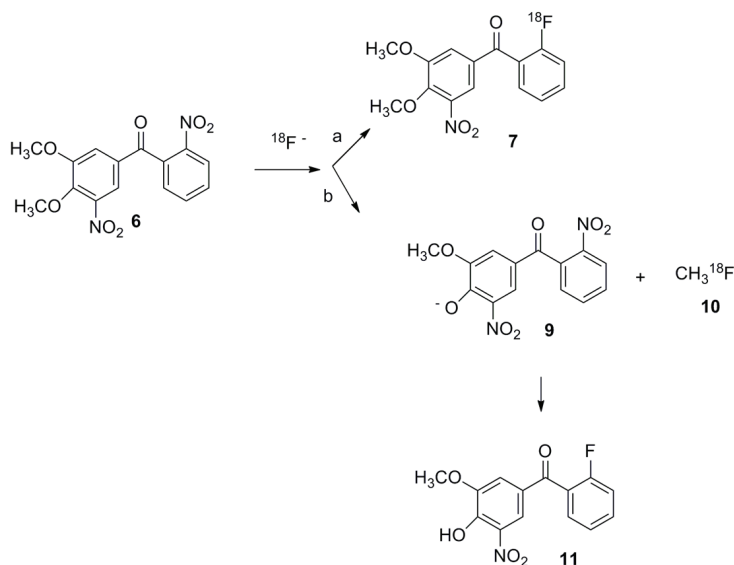
Nitro groups

Nucleophilic aromatic substitution by [18F] fluoride ion on an aryl nitro group has become one of the most useful labeling methods in PET chemistry [29-33]. A suitable leaving group, positioned on an aliphatic section of the target molecule, can be subjected to nucleophilic substitution conditions. Some groups, such as $-NO_2$, -OAr, or -OR, are not suitably reactive when present on an aliphatic carbon, but have been shown to work as leaving groups when present on an aromatic ring [34]. On the other hand, fluorination on halide containing aliphatic carbons has been shown to work well, but achieving reactivity of halide functionalized aromatic compounds requires harsh reaction conditions, such as high temperature and prolonged reaction times, producing low overall yields of the desired product [35-37].

Examples of using nitro aromatic compounds as precursors for radiofluorination are plentiful. One such example was in the development of a catechol-O-methyltransferase inhibitor, 3,4-dimethoxy-5-nitro-2'-[18F]fluorobenzophenone 7. This was done through nucleophilic aromatic
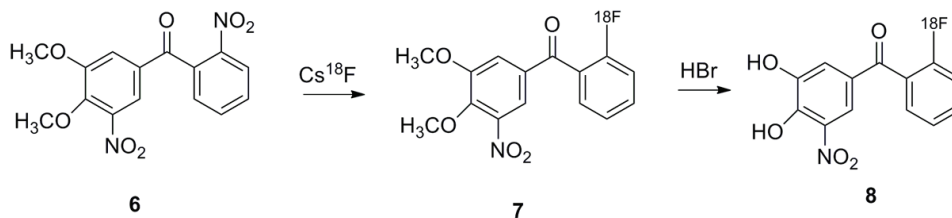
Figure 4. Synthesis of 3,4-dimethoxy-5-nitro-2'-[18F]fluorobenzophenone via nucleophilic aromatic substitution.

Figure 5. Production of [18F]fluoromethane during the fluorination of methoxy substituted benzophenone.

substitution of an aromatic nitro group using Cs18F [38]. The target product, 8, was then achieved through subsequent deprotection of the methyl ether groups using HBr (**Figure 4**). In this synthesis, a by-product was observed, which was found to be due to the nucleophilic attack of [18F]fluoride on the methoxy moiety ortho to the nitro group on the A ring of compound 6. The [18F]fluoromethane 10 and 4-hydroxy-3-methoxy-5-nitro-2'-[18F] fluorobenzophenone 11 were identified by radio-TLC and HPLC (**Figure 5**). The formation of by-product 10 and the corresponding oxygen anion are reasonable due to the stabilizing resonance structures of 9 produced by electrons flowing between the para ketone carbonyl and the adjacent nitro group.

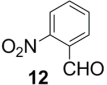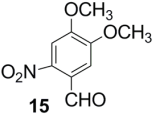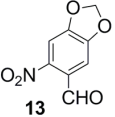This interesting observation was not reported in any previous work involving fluorination of cate-
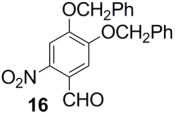
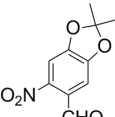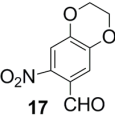chol substrates with [18F]fluoride such as in the labeling of 6-fluoro-DOPA, 6-fluoro-DA, or 6-fluoro-NE using 3,4-dialkyl protected catechol 6-nitrobenzaldehyde as precursor [39]. The formation of [18F]CH3F accounts for the low RCY of the desired product 8, which was only 10% of the radioactivity present at the end of bombardment (EOB). Interestingly, all the nucleophilic aromatic substitution reactions of this type were carried out using Cs18F, while other [18F] fluoride forms, such as N+Bu4 18F and K18F (Kryptofix 2.2.2), did not afford the desired products.

An additionally remarkable aspect of this study, which deserves a brief discussion, was the observation that the nitro group, ortho to the methoxy group, was never indicated to undergo substitution. Typically, [18F]fluoride displacements will only occur on rings that possess a suitable electron withdrawing moiety, such as a carbonyl located *ortho* or *para* to the leaving group. Extensive studies have been conducted in an effort to investigate to what extent the hydroxyl protecting groups actually play in controlling the reactivity of aromatic rings toward nucleophilic substitution of the 18F nucleophile (**Figure 6**) [39].

Radiofluorination yields were excellent when there were no electron donating groups on the ring (compound 12) and the RCY was still fairly good when catechols 13 and 14 were protected as 1,3-dioxolanes. However, while under the same conditions, the reaction suffered from low yields when alkyl-protecting groups were used (15 and 16). The position of a single methoxy group on the aromatic ring was also shown to have an effect on chemical yield; only a trace of

Compound	RCY	Compound	RCY
12	78%	**15**	23%
13	51%	**16**	24%
14	42%	**17**	0%

Figure 6. Radiochemical yields for radiofluorinations of various nitro-benzadehydes.

product formed (5%) when the methoxy group was positioned *para* to the nitro group. The yield improved (23%) when the methoxy moiety was *ortho* to the nitro group. Interestingly, 1,4-dioxolane 17, which is similar to compounds 13 and 14, was inert to nucleophilic substitution reactions. These yields could be explained and even predicted by comparing the ^{13}C NMR shifts of the nitro group containing aromatic carbon, which has a direct correlation to the electron density of the carbons of interest.

Trimethylammonium salts

Nearly a decade ago, aryl[^{18}F] fluorination via nitro precursors was considered the most popular method used in PET chemistry [40, 41]. With the need for greater reactivity at lower reaction temperatures radiochemists have begun to shift their focus onto the preparation of better leaving groups, such as aryltrimethyl ammonium salt precursors. This family of leaving groups is ideal for PET chemistry, with a decrease in the necessary reaction temperature, or an increase in the overall RCY, excessively large amounts of

radioactivity at the beginning of the reaction sequence can be avoided. The reduction in temperature allows for a lowering of the potential formation of non-radioactive by-products that would lower the specific activity of the product. This also opens up the possibility of producing products with nearly 100% incorporation and specific activities approaching the theoretical maximum [42].

The choice of the counter ion employed in the formation of the trimethylammonium salts has been shown to influence the speed of the displacement of the ammonium from an aromatic ring. It has been reported that aryltrimethylammonium perchlorate can be displaced via [^{18}F] fluoride ion attack, but decomposition of the precursor can occur at elevated temperatures making the wide scale use of these salts impractical for systems that require harsh labeling conditions [43]. An additional disadvantage of the perchlorate salts is the lengthy preparation required to employ them in these reactions.

Triflate salts were also found to be compatible with nucleophilic aromatic substitution using [^{18}F]fluoride ion in the presence of Kryptofix [2.2.2] using DMSO as the solvent [43]. The reaction time and temperature is quite low compared to other derivatives, but it appears to be ideal for some of the more demanding chemical structures. For example, some ester derivatives can simply not tolerate reactions using high temperatures while in the presence of a base [14]. During the course of designing and optimizing the method for the labeling of benzodiazepine receptor ligand 18, it was found that the labile trimethyl ammonium triflate salt affords a very suitable leaving group (**Figure 7**), even in the presence of sensitive esters that would normally be problematic under labeling conditions. It is believed that the non-nucleophilicity of the triflate anion in comparison with K_{222}/[^{18}F]fluoride helps to promote the reactions outcome. The overall RCY for the syn-
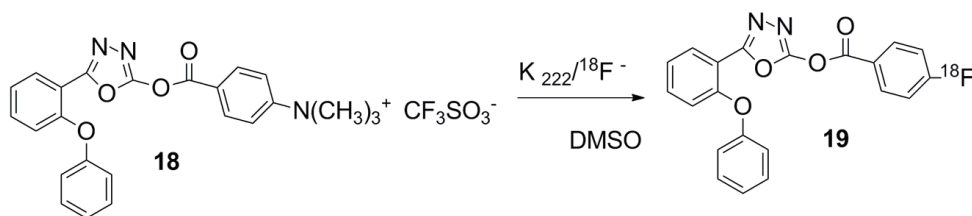
Figure 7. Fluorination in the presence of a sensitive ester derivative.
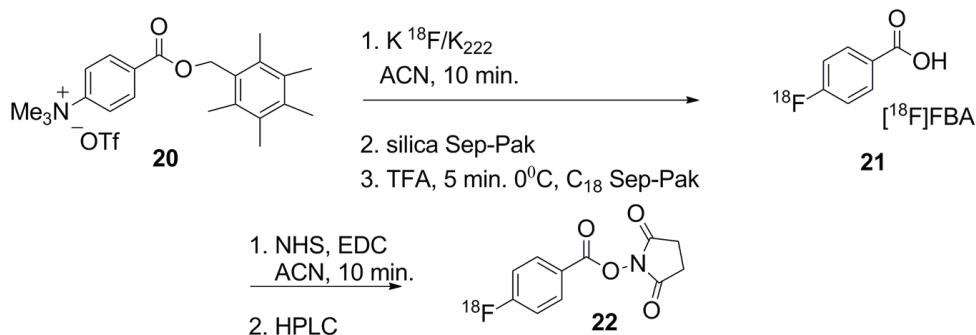
Figure 8. Production of [18F]SFB via production of [18F]FBA.

thesis of 19 was 75% after decay correction, which included purification via a C_{18} Sep-Pak™ cartridge.

Given the excellent ease of substitution by the [18F]fluoride ion at moderate reaction temperatures and the generally high RCYs of such reactions, trimethylammonium salt leaving groups allow for the production of reactive linkers for PET labeling of the most sensitive molecules, such as peptides, proteins and antibodies, all of which are either heat sensitive or chemically sensitive. The general features of these linkers are the presence of an aryl trimethylammonium moiety on one end of the molecule, while the other end possesses a functionality that can be used to take advantage of one of the many reactive species found on the surface or backbone of the biomolecules, such as thiols or primary amines. In all likelihood, the most well-known procedure using this type of radiosynthetic approach is that of the formation and reaction of N-succinimidyl-4-[18F]fluorobenzoate ([18F]SFB) [44]. Preparation of [18F]SFB begins with the formation of the intermediate molecule 4-[18F]fluorobenzoic acid ([18F]FBA) and is comprised of three total steps, therefore, high RCY labeling to form [18F]FBA is a step crucial in the sequence, since all other steps will suffer if the initial labeling does not go well. Fortuitously, it has been shown that the precursor trimethylammonium triflate and a variety of other ammonium salts can provide better RCYs and are, therefore, excellent precursors for the synthesis of [18F]FBA [45].

In the course of developing 18F-labeled insulin as a PET tracer, it was demonstrated that [18F] FBA 21 could be reliably produced using trimethylammoniumpentamethylbenzyl-

protected benzoic acid triflate 20 as a precursor [46]. The radiolabeling procedure entailed a two-step reaction sequence that included the labeling reaction followed by cleavage of the pentamethylbenzyl-protecting group using trifluoroacetic acid (TFA), which resulted in the benzoic acid functionality (**Figure 8**). The decay corrected RCY for the labeling step alone was found to be 76% ± 9% (n = 10). However, during the deprotection step a significant loss of activity occurred (between 50 and 80%) during the evaporation of the residual TFA. In order to avoid this loss of activity an alternative TFA removal approach, employing C_{18} Sep-Pak™ adsorption followed by elution of the desired product, was developed to overcome the loss of activity observed in the earlier protocol.

In addition to [18F]SFB, which takes advantage of the presence of reactive primary amines, an alternative linker, N-[6-(4-[18F] fluorobenzylidene)-aminooxy-hexyl]maleimide ([18F]FBAM), has been developed to take advantage of the presence of any reactive thiols present on biomolecules [47]. Preparation of this compound is accomplished via the fluorination of 4-N,N,N-trimethylammoniumbenzaldehyde triflate with K_{222}/[18F]fluoride at the moderate temperature of 120 °C for a period of 15 minutes, giving a RCY of up to 80% without the need for any purification. The labeled 4-fluorobenzaldhyde was then carried on and coupled with N-(6-aminohexyl)maleimide to produce the desired product, which needs to be purified via semi-preparative HPLC giving an overall purity of 98% or better for the end product.

When considering the design and implementation of feasible fluorinated linker molecules, PET chemists must take into account the time con-
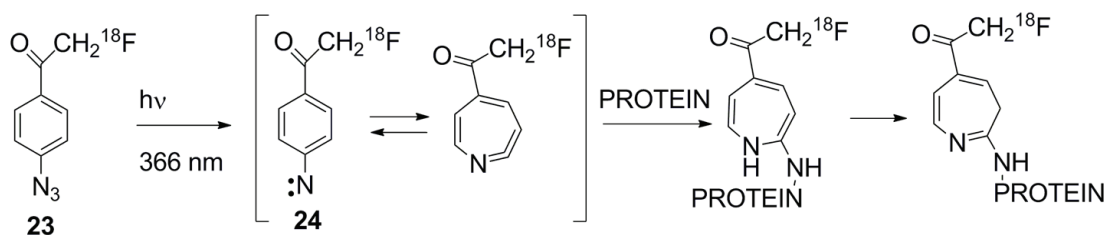
Figure 9. Use of UV light to produce an aryl nitrene from an aryl azide for the purpose of conjugation to a protein target.

straints of working with a relatively short lived isotope and the number of synthetic steps employed. In this particular application, microwave-assisted techniques hold great potential for improving the reaction time and as a result the overall RCY. In this approach, the reaction time can be cut from, worst case scenario, hours to, best case scenario, a few minutes, which has been demonstrated for the radiosynthesis of [18F]SFB [48]. Starting from t-butyl protected 4-trimethylammonium-benzoic acid triflate, [18F]FBA was synthesized based on the microwave-induced one pot reaction of [18F]FBA by a nucleophilic 18F-fluorination with acidic hydrolysis using TFA. This one-pot approach provided [18F]FBA in a RCY of 70-90% with a radiochemical purity of greater than 95%. Further conversion of [18F]FBA into [18F]SFB was accomplished in one step as already shown in **Figure 8**. Finally, [18F]SFB was obtained in a decay-corrected RCY of 44-53% and radiochemical purity of >95% within 40 minutes after the EOB.

An additional example of microwave induced heating was shown in the production of 2-(4-[18F]fluorophenyl)benzimidazole, an important building block for many endogenous and pharmaceutically active compounds [49]. In this work the synthesis of 2-(4-[18F]fluorophenyl) benzimidazole was accomplished by the nucleophilic radiofluorination of 4-trimethyl-ammonium -benzonitrile-trifluoromethanesulfonate followed by alkaline hydrolysis of the nitrile producing 4-[18F]fluorobenzoic acid, all with traditional heating. The decay corrected RCY over the two steps was 82% ± 10% and the radiochemical purity was greater than 99%, determined using radio-HPLC. The 4-[18F]fluorobenzoic acid then went through a cyclocondensation with 1,2-diaminobenzene using polyphosphoric acid under microwave assisted heating. It is worth noting that when this reaction was performed with

conventional heating no product was detected after 24 h at 100 °C. Examples for the preparation of new and existing linker molecules continue to appear in the literature and have thus far continued to show great promise for the functionalization of both small and large molecular target compounds [50-53].

Regioselective radiolabeling of small molecules is easily accomplished directly onto the compound of interest via a suitable activating group. However, this approach is still far from reality with biological molecules such as peptides, proteins, antibodies, their fragments, or any heat-sensitive entities. In addition, modifying these analogs with activated moieties serving as precursors for PET labeling is impractical due to the complexity of said molecules. Therefore, it has been found to be advantageous to develop radiolabels that can be attached to the molecule of interest via a suitable linker. Conceptually, an ideal linker for PET chemistry should have a leaving group on one end that can be used for nucleophilic substitution by a radionuclide and an activated moiety on the other end for bioconjugation. As has already been described, several strategies have been developed for this approach including linkers by acylation, amidation, imidation, and alkylation [54-57]. In order to devise a more efficient method of radiolabeling proteins or heat sensitive entities, a number of studies have focused on photo chemistry as a means for bioconjugation reactions; as shown in **Figure 9**, a demonstration of photochemical conjugation between [18F] arylazide 23 and a protein via a single step synthesis using UV light at 366nm [58]. However, low labeling efficiency has been reported due to the short lifetime of the intermediate [18F] arylnitrene 24. For additional information on the recent advances in the field of linker chemistry for [18F]fluoride labeling, see Toyokuni's work
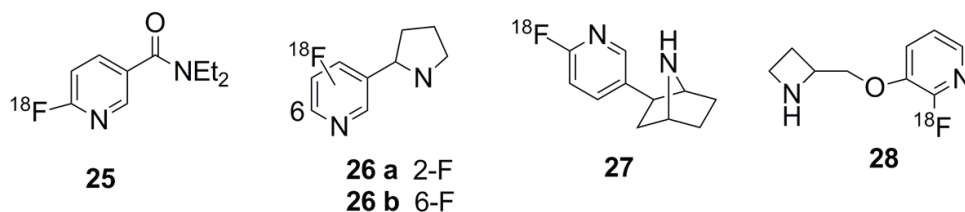
Figure 10. Representative examples of [18F]fluoropyridine derivatives.

Temperature (°C)	Substituents (X)	Reaction time (min)		
		5	10	20
120	Cl, Br or I	0	0	0
	NO₂	11	76	82
	N⁺Me₃	81	87	91
150	Cl	1	3	23
	Br	1	16	25
	I	0	0	1
	NO₂	52	85	92
	N⁺Me₃	89	89	90
180	Cl	11	28	57
	Br	56	60	87
	I	2	5	19
	NO₂	77	88	89
	N⁺Me₃	88	91	92

Figure 11. Reaction yields for a variety of substituted pyridines.

[59].

Nucleophilic heteroaromatic

In contrast to homoaromatic and aliphatic compounds, nucleophilic substitutions of [18F] fluoride ion onto heteroaromatic compounds are usually less voracious [60]. One of the typical syntheses of heteroaromatic PET probes is that of 2-[18F]fluoropyridine derivatives, which have been reported for the preparation of ana-

logues of key radiopharmaceutical products, such as 6-[18F]-fluoronicotinic acid diethylamide 25 (**Figure 10**). A yield of 40% can be achieved when using a 2-chloropyridine derivative and [18F] fluoride ion in acetamide at 200°C [60, 61]. The preparation of 2- and 6-[18F]fluoronicotine 26a and 26b from the precursors 2- and 6-bromopyridine using [18F]CsF have also been previously reported [62]. In order to gain information concerning the pharmacological properties of neuronal nicotinic acetyl choline receptors (nAChRs), two nAChRs PET probes 27 and 28 were synthesized via nucleophilic displacement from the 2-pyridine activated moieties, where 27 was a 2-ammonium salt and 28 utilized a 2-nitro precursor [63, 64]. The properties pertaining to pyridine fluorinations were intuitively understood from these studies, however it was only fairly recently that a full study of the reaction conditions for 18F labeling of pyridines was actually done [60].

The influence of the leaving group in the second position of pyridine was investigated under several reaction conditions, i.e. differing solvents, temperatures, and reaction times (**Figure 11**). Incorporation of 18F through either the NO₂ or N⁺Me₃ starting materials provided better RCY when compared to their halide counterparts. A very impressive incorporation yield was observed for the trimethylammonium substituent at 5 minutes, independent of the reaction temperatures attempted. Comparable yields were observed for the nitro moiety when a longer reaction time was applied.

Precursors using the bromo and chloro derivatives were not reactive at 120°C and provided low yields at elevated temperatures and extended times. It is surprising that the iodo derivative leaving group was inert at 120°C and 150°C under 20 minutes of reaction time while the reaction provided very low yields at 180°C and a reaction time under 20 minutes (19%). It is important to note that the incorporation yields for most leaving groups were sufficient in 20 minutes at 180°C, with the exception of the iodo derivative.

The radiolabeling of heteroaromatic compounds is yet another group of compounds that can benefit from a decrease in both reaction time and temperature, which leads to a subsequent increase in RCY. This can be afforded by the adoption of microwave-assisted heating. The typical RCYs observed for the labeling reactions of heteroaromatic compounds are usually between 5-35% by conventional heating and 20-75% by microwave irradiation. Some of the early examples of heteroaromatic substitutions employing chloro- and bromo-analogs as leaving groups included compounds such as 6-chloronicotinic acid and 2-, 6-bromonicotine [65, 66]. As a potential nicotinic acetylcholine receptor agonist, exo-2-(5'-pyridyl)-7-azabicyclo-[2.2.1]heptane was ^{18}F labeled via nucleophilic substitutions on the 2'-bromo, 2'-iodo and 2'-nitro activated precursors in an effort to optimize the reaction parameters and gain the best possible RCY. Synthetically, the target molecule was obtained from the corresponding boc-protected precursors using [^{18}F]/K$_{222}$ in DMSO by heating from 150-180 °C over 10 minutes and microwave irradiations at 100 W over a time frame of 1-3 minutes [67]. In these experiments, the RCY with respect to the [^{18}F]fluoride ion were 51% for the bromo-derivative and 29% for the nitro-derivative as measured by radio-TLC. A lower labeling reactivity was observed for the iodo-derivative and as a result not fully explored. With microwave activation at 100 W, an improved RCY was observed for both bromo- and nitro-substituted precursors, producing 72% from the bromo precursor in 2.5 minutes and 45% from the nitro precursor in 1.5 minutes.

In an effort to determine the extent of reactivity and the extent that the location of the leaving group has on reactivity, a series of experiments were done with a variety of known leaving groups (Cl, Br, and NO$_2$) in either the 5- or 6-position of the pyridine [68, 69]. What was observed was that the yields of the labeling reactions increased as the reaction time approached 10 minutes up to 26% for the 6-chloro - and 63% for the 6-bromo. High incorporation yields (~90%) were observed at 3 minutes for the 6-nitro- derivatives. However, under all reaction conditions, the 5-substituted derivatives were completely unreactive. It should be noted that when considering a leaving group for the substitution reaction at the ortho-position, results from Karramkam et al indicate that the order of reactivity for the leaving groups toward the ortho fluorination of a pyridine derivative follows the general trend of NO$_2$>Br>Cl.

Pyridines are not the only heteroaromatic compounds to undergo rigorous examinations in an effort to obtain a radiolabeled product, 1,3-thiazoles have also been explored [70]. Fluorination at the 2-position was shown to be possible under both traditional heating and microwave induced heating techniques using bromo, chloro and iodo as leaving groups. In all cases, the microwave-induced heating was shown to give a higher yield of the desired product over the conventional heating.

Electrophilic fluorination

Fluorine-18 aryl labeling can be achieved by either nucleophilic substitution or alternatively by an electrophilic approach which may be the only means of introducing a fluorine atom, such as in the case of a very electron rich aromatic species. The downside of electrophilic fluorination with [^{18}F]F$_2$ is that the products that are produced have a maximum specific activity of no greater than 50% of the theoretical maximum, due to the nature of the [^{18}F]F$_2$ reagent containing only one of the desired ^{18}F atoms per molecule. In reality, the maximum specific activity that can be obtained is orders of magnitude less than 50% of theoretical due to isotopic dilution from the addition of cold F$_2$ gas. The direct electrophilic radiofluorination of an aromatic precursor with a trimethylstannyl substituent as a leaving group has been widely used in the preparation of ^{18}F-labeled amino acid derivatives, such as [^{18}F]fluoro-L-DOPA ([^{18}F]FDOPA), a widely used PET tracer for imaging dopaminergic metabolism and a variety of tyrosine derivatives [71, 72]. This simple and time efficient procedure has been quickly employed in the

$X = HSO_4^-, CF_3CO_2^-, CF_3SO_3^-, TfO^-, BF_4^-, HO^-, Cl^-, IO_3^-, Br^-$
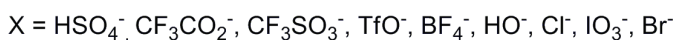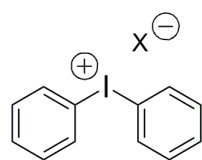
Figure 12. Diaryliodonium salt with representative known counterions.

development of additional types of PET tracers.

The synthesis of 6-[18F]fluoro-L-DOPA was first developed at UCLA via radiofluorodestannylation using either [18F]F_2 or [18F]CH_3COOF, which, thus far has been reported as the most suitable for the automated preparation of 6-[18F]Fluoro-L-DOPA [73-75]. Interestingly, the radiochemical reaction occurred at room temperature in only 10 minutes to afford 26% RCY after decay correction. The product was found to be 99% chemically pure. In addition, no racemization was detected by chiral HPLC analysis. The efficient radiosynthesis of 3-O-methyl-[18F]fluoro-DOPA ([18F]OMFD) has also been reported using this same kind of methodology [71]. The total preparation time of [18F]OMFD after EOB was about 50 minutes while a 20-25% decay-corrected RCY was obtained with 98% chemical purity. An additional reagent that has been explored is 6-[18F]fluoro-L-*m*-tyrosine ([18F]FMT), which represents an alternative substrate for measuring the activity of the enzyme aromatic L-amino acid decarboxylase (AAAD). The reactivity of two unique precursors, both possessing a trimethyltin leaving group, towards electrophilic 18F labeling of [18F]FMT were compared by Van-Brocklin *et al* and identical yields were produced [72]. Decay corrected RCYs of [18F]FMT were about 25%, which are similar to those results reported from other researchers [76]. The chemical purity was determined by HPLC as greater than 96%.

Diaryliodonium salts

The use of diaryliodonium salts represent the newest method for [18F]fluoride labeling of aromatic compounds compared to previously discussed methods. What stands out about this class of compounds is the excellent nucleofugality of the phenyliodonio group, which has shown a leaving group ability of about 10^6 times greater than that of an alkenyltriflate. This enhanced leaving ability allows for the efficient placement of [18F]fluoride [77, 78]. Generally,
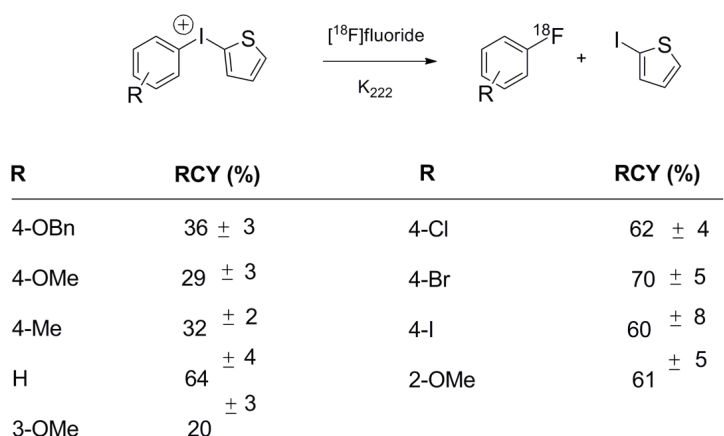
diaryliodonium salts are air stable, crystalline solids that are slightly sensitivity to light. Counterions associated with the salts are typically triflates or tosylates, but a wide variety of anions can be employed (**Figure 12**).

Given that nucleophilic attack can occur on either of the aromatic carbons alpha to the hypervalent iodine, studies have shown that both electronic and steric affects dictate which carbon will be functionalized. Grushin *et al* have shown that the carbon with the lowest electronegativity (i.e. most electron-poor) will preferentially be attacked [79, 80]. On the other hand, a variety of studies have shown that the carbon possessing a bulky group in an adjacent position will undergo attack [81, 82]. Having these two characteristics available for manipulation allows researchers to develop a variety of precursors specifically designed to produce the labeled product of interest. Ross *et al* demonstrated these characteristics by recording the RCY of reactions involving [18F]fluoride in the presence of kryptofix [2.2.2] with different iodonium salts having various electronegative groups on one aromatic ring while holding the second ring constant (**Figure 13**) [83].

Carbon-11 labeling methodologies

Carbon-11 (11C) is one of the most diverse nuclides used in today's PET chemistry world due to the fact that 11C can be produced and rapidly transformed into a large variety of useful synthons. This allows for the production of an ever expanding catalog of new and innovative imaging agents [84]. Production of 11C is accomplished through the proton bombardment of 14N gas with trace amounts of either hydrogen, for the production of [11C]CH_4, or oxygen, for the production of [11C]CO_2. From these two synthons, one can perform the necessary chemistry in order to obtain the desired form of 11C they wish to use for labeling reactions (**Figure 14**).

After 18F-labeled probes, one can make the ar-

R	RCY (%)	R	RCY (%)
4-OBn	36 ± 3	4-Cl	62 ± 4
4-OMe	29 ± 3	4-Br	70 ± 5
4-Me	32 ± 2	4-I	60 ± 8
H	64 ± 4	2-OMe	61 ± 5
3-OMe	20 ± 3		

**Figure 13.** Radiochemical yields for a variety of substituted diaryliodonium salts.
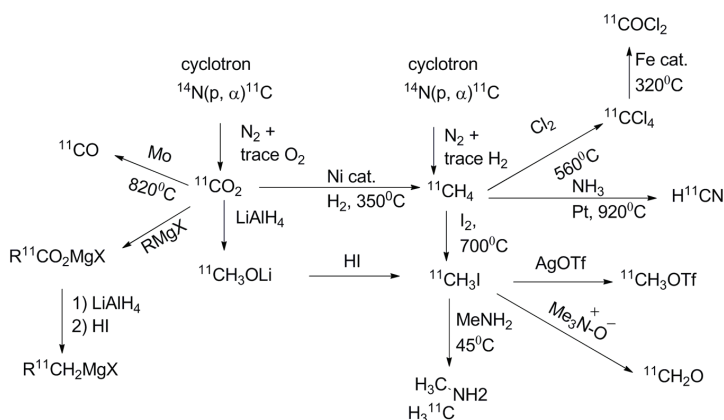
Figure 14. Schematic showing the wide variety of different synthons that can be produced for the incorporation of ^{11}C into a target molecule of interest.

gument that ^{11}C-labeled probes are the next most popular nuclide currently used in PET imaging. [^{11}C]Methyl iodide is frequently used as a ^{11}C-precursor due to its ease of production and handling. Several compounds suitable for labeling with [^{11}C]methyl iodide are common among biologically active substances, such as nicotine, deprenyl, 3-quinuclindinyl benzilate (QNB), and a variety of others (**Figure 15**) [85-87]. When radiochemical reaction times and high yields are critical, a more reactive source of ^{11}C, such as [^{11}C]methyl triflate, has been found to be essential. The preparation of [^{11}C]methyl triflate can be accomplished by simply combining [^{11}C] methyl iodide with silver triflate at an elevated
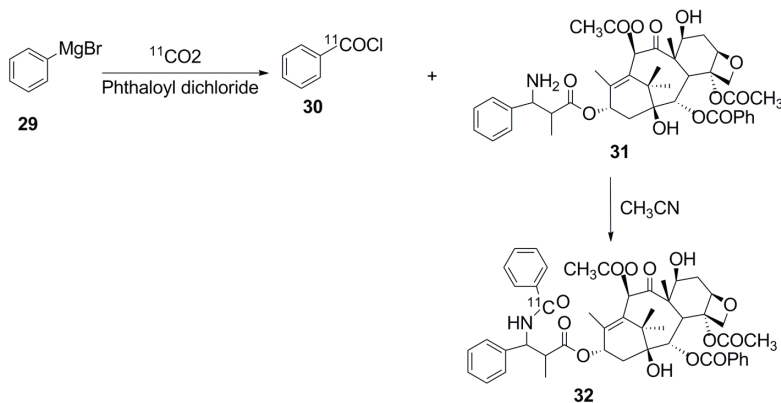
temperature. Since the introduction of [^{11}C]methyl triflate labeling methods several biologically active compounds have been prepared in high radioactive quantities (80-170 mCi), thereby making multiple PET studies in human subjects possible [88]. The rate of alkylation onto pharmaceutically active compounds using [^{11}C] methyl triflate was carefully compared to that of [^{11}C]methyl iodide. It was been shown that N-methylation using [^{11}C]methyl triflate provided consistently higher RCY in more efficient times with moderate heating in comparison to the [^{11}C]methyl iodide attempts [89].

Labeling to form ^{11}C-containing molecules from a variety of different precursors is important not only in the number of compounds that can be labeled with ^{11}C, but also by creating the possibility of labeling a given compound at different positions [90, 91]. Labeling molecules of interest with ^{11}C-containing carbonyls is another important feature that facilitates the availability of PET probes for study. [^{11}C]carboxylation employing the Grignard reaction between alkylmagnesium halides and [^{11}C] CO_2 has been demonstrated for the production of myocardial fatty acids with modest yields [92]. It is worth mentioning that this specific example of [^{11}C]carboxylation was carried out in THF at room temperature, which provides an alternative approach for a broad range of lipophilic and heat sensitive compounds.

Another tangible example demonstrating the versatility of ^{11}C labeling in PET chemistry lies in the conversion of Paclitaxel, an effective anti-cancer drug against solid tumors, into a cancer-imaging agent. [^{11}C]Paclitaxel 32 was prepared via a multi-step synthetic route with the [^{11}C] moiety incorporation being the last step, which was accomplished by reacting [α-^{11}C]benzoyl chloride 30 with the primary amine precursor of Paclitaxel (31) (**Figure 16**) [93]. The time required to obtain the product from the EOB to the purification, including a formulation step, was an astonishingly low 38 minutes. The reaction
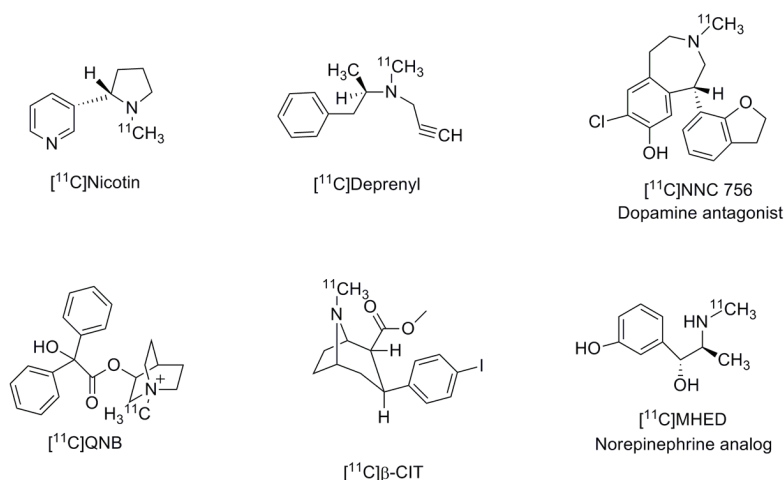
Figure 15. A sampling of biologically active compounds that have been labeled with [11]C.

Figure 16. Synthesis of [^{11}C]Paclitaxel using [^{11}C]CO_2 as the source of [11]C.

phile and a zero valent palladium catalyst can be employed for making a spectrum of important compounds such as amides, carboxylic acids, esters, aldehydes and ketones [94, 95]. Amides are particularly important moieties given their intrinsic existence in virtually all natural products, as well as in bioactive pharmaceutical compounds. The synthesis of amides utilizing carbon monoxide in a multicomponent reaction was found to be compatible with PET chemistry developed by Murahashi *et al* [96]. Since then, many efforts have been put forth for the convenient production of [^{11}C]CO in an effort to make this reagent synthetically viable. One of the most difficult tasks is finding an efficient method of trapping [^{11}C]CO in a reaction medium. If the [^{11}C]CO is not trapped in a medium the subsequent loss of gas leads to low reaction yields. To tackle this problem, a fully automated version of a micro-autoclave system that traps [^{11}C]CO as a precursor with high efficiency has been developed and implemented to show functionality [85]. For most cases, the labeling procedure is short (15 minutes) with reports of high specific activities (27 Ci/mmol) and radiochemical purities of the final products exceeding 98%.

provided a remarkable specific radioactivity of 1349 mCi/mmol and a decay corrected RCY of 7% with 99% radiochemical purity.

Despite the short half-life of ^{11}C PET probes they constitute a large number of the currently developed useful reagents for imaging studies. The key reason ^{11}C probes are so widely used lies in the fact that incorporation of ^{11}C into a precursor does not affect any of the key properties, such as binding affinity, to the *in vivo* targets. Moreover, ^{11}C generated from carbon monoxide, which is an easily obtainable and very active synthetic moiety, facilitates versatile chemical syntheses. For example, a three-component synthesis involving carbon monoxide, a nucleo-

Transition metal labeling methodologies

Among the various and available PET radioisotopes, ^{64}Cu and ^{68}Ga offer many advantages over other traditionally used isotopes [97]. With a half-life of 12.7 hours, ^{64}Cu is compatible with *in vivo* kinetics to investigate biodistribution and metabolism of compounds of interest using PET imaging. Additionally, this long half-life radioisotope has been shown to be useful for tracking cell migration and their cellular fate *in vivo*. The isotope also allows for serial imaging for up to several days [98]. A major downside of ^{64}Cu lies in the need for a cyclotron equipped with a solid
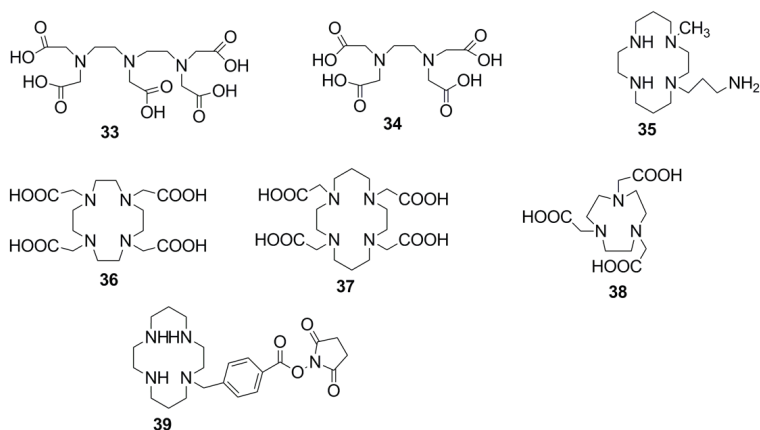
Figure 17. Representative examples of linear chelators and macrocyclic polyaminocarboxylates.

target for its formation via the nuclear reaction $^{64}Ni(p,n)^{64}Cu$, which is one of the only methods used that is capable of producing large quantities of ^{64}Cu with high specific activity [99]. In this way, ^{68}Ga (68 minute half-life) holds an advantage over ^{64}Cu since it is commonly generator produced from the decay of ^{68}Ge (275 days). This allows modest sized hospitals to obtain the isotope on a routine and reliable timeframe [100].

The challenge in the implementation of metal radioisotopes lies in the design of chelating agents that have the ability to not only retain the metal *in vivo*, but either become the targeting agent or be attached to a known targeting agent without adversely affecting the targeting properties or kinetics. While the synthetic chemistry is usually straightforward, the design that enhances the physical binding of the chelators to the metallic radionuclides often requires extensive knowledge of the metal selectivity and metal-chelator stability under physiological conditions. Early studies have identified diethylenetriaminepentaacetic acid (DTPA, 33) and ethylenediaminetetraacetic acid (EDTA, 34) (**Figure 17**) as potential bifunctional chelators for both copper and gallium radioisotopes [101].

The observed rapid dissociation of copper from common scaffolds prompted the search for more efficient and stable chelators [102]. It has been found that the dissociation rate of copper from the known cyclic polyamine chelates is

extremely slow when compared to the non-cyclic polyamine chelates; in addition, studies have shown that these complexes are kinetically stable under biological conditions. This observation has been confirmed by several studies that showed ^{64}Cu complexed with tetraaza monoamine cyclam 35 loses less than 0.5% of the copper after 24h of incubation in human serum at 37 ° C. Incubation for periods up to 48h in 1mM EDTA showed no significant loss of ^{64}Cu, however there was 100% loss of copper using the acyclic homologue N,N'-bis-(aminoethyl)-propylenediamine complex under the same conditions after just 2 minutes [97, 103].

Since the previous studies, more convenient bifunctional chelators with amino reactive functional groups have been developed, such as compound 39 for conjugation with bioactive ligands. The advantage of this type of radiolabeling is that biomolecule-conjugate scaffold precursors can be prepared and stored without any shelf life decomposition. Therefore, biomedical scientists can label the precursor scaffolds with the ^{64}Cu isotope without using reaction conditions that need advanced chemistry
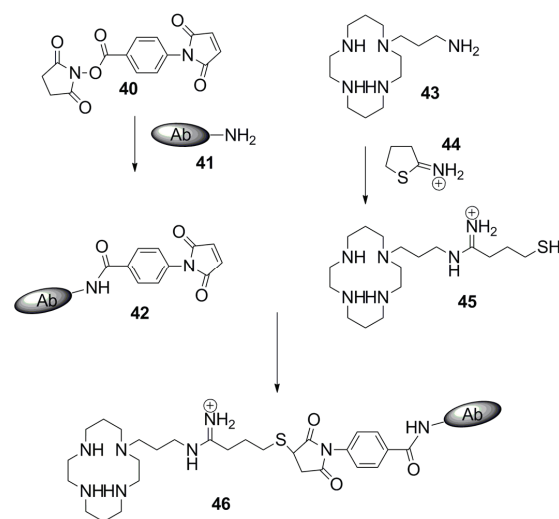
Figure 18. Conjugation of an antibody (Ab) with a suitable cyclam to afford a stable ^{64}Cu-labeling precursor.

skills. As shown in **Figure 18**, an antibody derivative 41 can easily be conjugated into a commercially available bifunctional linker 40 before attachment to the modified cyclic polyamine chelator 45. The precursor 46 can be purified, stored and when needed, be available for labeling with ^{64}Cu at any time in the future.

In order to simplify the bioconjugation process, the macrocyclic polyaminocarboxylates 36-38 (**Figure 17**) were developed. Due to their great application in PET imaging, the activated ^{64}Cu-polyaminocarboxylates, when combined with peptides and antibodies have been widely used to image tumor lesions [104-106]. For more information on the superior characteristics of cross bridged cyclams compared to DOTA complexes *in vivo*, refer to an excellent study done by Anderson and co-workers [107].

Chemistry of optical imaging probes

Introduction to optical imaging

It has been known for quite some time that natural objects such as phosphorus-containing compounds or living subjects like fireflies, insects, and marine organisms have the ability to emit light. However, imaging using a source of fluorescent light for *in vivo* applications is an emerging technique, one that has been developed over the past decade. With the advent of laser technology and sophisticated optical devices the sensitivity, selectivity and simplicity of these devices has made the use of fluorescent imaging methods more attractive. Recently, several near-infrared (NIR) fluorescent probes have shown great promise for *in vivo* imaging of biological targets such as somatostatin receptors, osteolastic activities and proteases [108-118]. NIR light spans the wavelength range from 700-900 nm. Therefore, NIR light is more ideally suited for *in vivo* imaging than light in the visible spectrum. NIR light is able to penetrate tissue more efficiently compared to visible light that is easily scattered and absorbed by tissue [119]. Tissue absorption becomes weaker for wavelengths in the NIR region while scattering also decreases with increasing wavelength. Consequently, molecular beacons in the NIR range may provide enormous potential for non-invasive *in vivo* applications. In this section of the review we will discuss a few major families of dyes that have useful applications in molecular imaging including cyanine, rhodamine and oxazine dyes.
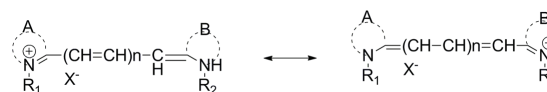

Figure 19. General structure of a cyanine dye, shown with the alternatively drawn resonance structure.

Preparation of cyanine dyes

Cyanine dyes are a major class of dyes that have been used in the textile, optical media and Xerox industries. More recent applications have been found in the molecular imaging field. Although there are several types of cyanine dyes, the general structure is composed of two nitrogen-containing heterocyclic rings joined by a conjugated chain of carbon atoms, as shown in **Figure 19**. There have been several review articles recently written on the synthesis of cyanine type molecules that demonstrate a variety of synthetic approaches, dye properties and their potential *in vivo* applications [120-124]. With the advent of molecular imaging, never before has so much effort been put forth to create biologically compatible cyanine dyes fitting essential criteria such as water solubility, quantum yield, toxicity, stability, and most importantly, NIR capabilities. In this section, we focus our discussion on the current methods of modification of cyanine dyes to be used for molecular imaging.

Preparation of methine cyanine dyes can be accomplished through the condensation between an active methyl-containing ring with an unsaturated moiety. The unsaturated moieties can be orthoesters, squarain derivatives or aldehydes when an aldol condensation reaction is used. For dyes with longer absorbance, a pentadienyl aniline salt can be used [125-128]. Use of this kind of condensation reaction allows the chemist to create either symmetrical or asymmetric dyes since the reaction can be controlled in a stepwise manner [129]. What is truly unique about cyanine dyes is that their absorbance and emission profiles can be predicted and fine-tuned by altering either the unsaturated carbon on the methines or the heterocyclic aromatic end rings. To clarify this notion, we would like to first start with the synthesis of a Cy3 dye by Konig *et al* from the beginning of last century. The synthesis of the Cy3 dye was achieved by condensation of a reactive quaternary ammonium salt 47 with a suitable orthoester in the presence of sodium tetra-
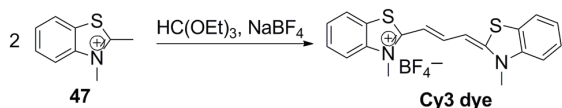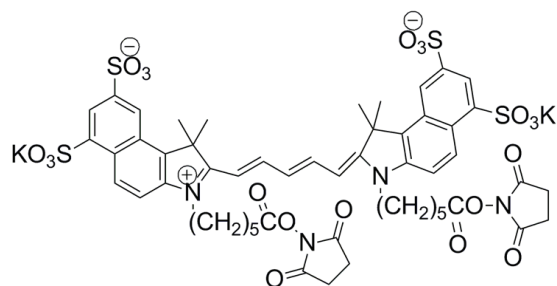
Figure 20. Synthetic scheme for the preparation of a Cy3 dye.
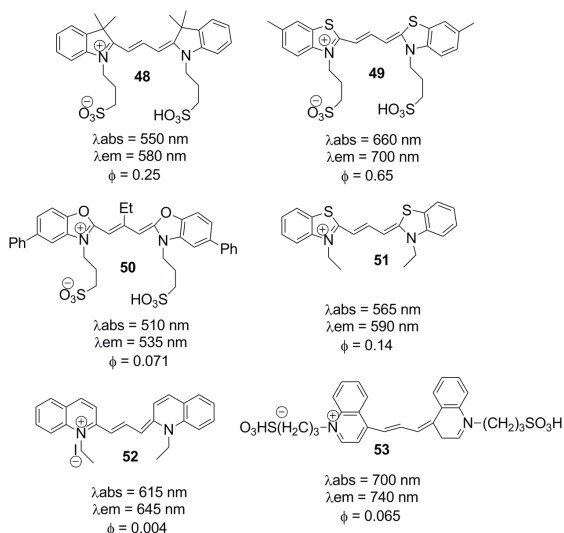
Figure 21. A variety of cyanine dyes that have been developed with their characteristic absorption and emission wavelengths (labs and lem respectively) and quantum yields (f).

Figure 22. Cy5 dye developed by Waggoner and co-workers for the purpose of labeling biomolecules.

fluoroborate. The blue-violet prism product was collected by recrystallization, producing an overall 70% yield (**Figure 20**) [130]. This type of reaction has become the model for preparing a number of important types of trimethine dyes [131, 132].

Over the many years of cyanine dye development, there have been several novel heterocyclic ring systems synthesized and studied (**Figure 21**). It has been generally observed that cyanine dyes derived from benzothiazole and indole rings have similar absorption (labs) and emission (lem) profiles. The quantum yields (f) of both dyes are also comparable and higher than other types of ring systems such as oxacarbocyanine 50, 2,2'-quinocarbocyanine 52, and 4,4'-quinocarbocyanine 53 [133]. It is worth noting that the electronic effect plays a very important role in the development of dyes in the NIR region. As an example of this concept, compound 49 is roughly the same size as 48 and

51; however, the electron donating methyl group of 49 has stabilized its ring system. As a consequence, it possesses a bathochromic shift of about 100 nm when compared to the other types. Structurally, increasing the number of carbons in the methine analogues, rather than the size of the aromatic ring system, tends to determine the bathochromic shift of cyanine dyes. For each double bond increased in the methine bridge, there will be an increase of about 100 nanometers in the wavelength versus an increase of only about 20 nanometers for every additional aromatic ring [134]. A practical extension of the cyanine bridge was developed using the condensation between an indole ring with malonaldehyde dianilide and glutacone dianilide to form Cy5 and Cy7 dyes respectively. In an elegant approach, Waggoner *et al* first demonstrated the power of chemistry in tuning the wavelengths of fluorescent dyes for *in vivo* imaging through the development of Cy5 dyes for the purposes of labeling biomolecules. Moreover, they were also able to overcome the hydrophobic nature of the long unsaturated system contained within the dye by incorporation of sulfonyl groups on the aromatic rings. This effectively helps to reduce the observed amount of dye aggregation under aqueous conditions (**Figure 22**) [128, 135, 136].

Despite these general guidelines, various limitations do exist which effectively hinder the development of long wavelength fluorescent dyes. An example of one such limitation is that the stability of cyanine dyes becomes a concern when the number of methine carbons linking the aromatic end groups together becomes greater than or equal to seven. Although there is no clear mechanistic explanation, the generally accepted theory postulates that long polymethine bridges might become unstable due to twisting, thus the
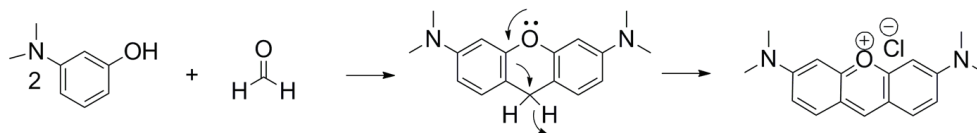
Figure 23. Synthesis of a simple rhodamine dye derived from 3-diethylaminophenol and formaldehyde.

dyes decompose easily during storage. In order to stabilize this class of NIR dyes, it becomes necessary to incorporate some of the methine groups into rings as a method of gaining stability. Reynolds *et al* was the first to synthesize a variety of stable heptamethine cyclic dyes and to thoroughly characterize the stability of the cyclic polymethine-containing cyanine dyes [137]. It was found that the presence of a central ring not only increases stability, but also results in a larger bathochromic shift compared to dyes with linear structures. Dyes with the central methine bridge derivatized as five-member rings absorb at longer wavelengths than those with six-member rings. This work demonstrated that all cyclic polymethine-containing dyes exhibit several orders of magnitude greater stability when compared to linear dyes. Additionally, the electronic effect contributed by some substituents was observed to have a greater effect on both the bathochromic shift of the cyanine dyes and their stability. For example, replacing the oxygen heterocycle with a sulphur heterocycle increased the bathochromic shift by 88 nanometers and nearly doubled the relative stability of the dye.

Another criteria that must be taken into account when designing fluorescent dyes for biological applications is the ability of the dyes to be modified with functional groups; allowing for the possibility of the dye to be attached to biomolecules for direct fluorescence detection. However, the practical synthesis of NIR cyanine dyes with reactive functional groups as an intermediate is challenging and not straightforward [138]. Currently, most dyes are designed to have amine or thiol reactive functionalities, usually N-hydroxysuccinimide or maleimide intermediates respectively. Since the conjugation step rarely goes to total completion, the purification of the desired product requires high performance liquid chromatography or size exclusion chromatography.

Preparation of rhodamine and oxazine dyes

The most popular agents for the labeling of bio-
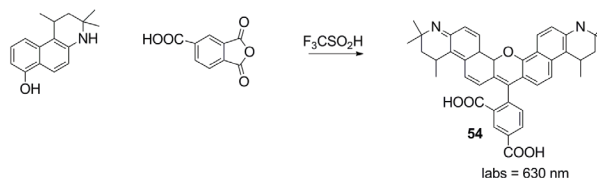
Figure 24. Synthesis of carboxylic acid functionalized rhodamine dye.

molecules for analytical staining, biological staining, antibody binding studies and photoswitching technologies are the rhodamine and oxazine dyes, both of which can be synthesized in a similar manner [139-141]. Rhodamine dyes are prepared by the condensation reaction between two molecules of *m*-diethylaminophenol with formaldehyde, followed by oxidation with ferric chloride in hydrochloric acid (**Figure 23**). In more elaborate work, rhodamine dyes are functionalized with carboxylic acid groups as handles for bioconjugation via a condensation process between an activated *m*-aminophenol or a 6-amino-naphthalen-1-ol derivative with phthalic anhydride (**Figure 24**) [142]. With the amino group making the ring system more rigid, compound 54 becomes more stable than the free amino counterpart and, as a result, has a better quantum yield.

In terms of molecular imaging, manipulation of the electronic effect in an effort to obtain a NIR feature without expanding the size of the dye, thus reducing the steric hindrance and hydrophobicity in a biological assay, is a crucial development. Similar to rhodamine dyes, oxazine dyes can be synthesized by replacing the central carbon of rhodamine with nitrogen, which exemplifies the previous concept. Nitrogen insertion results in a molecule that exhibits longer absorbance and emission wavelengths [143]. The central nitrogen atom serves as a sink for the π-electrons, causing a wavelength shift of about 80-100 nanometers towards the NIR region. Oxazine dyes have been traditionally synthesized by condensation of nitrosoaniline derivatives with a phenol in the presence of perchloric
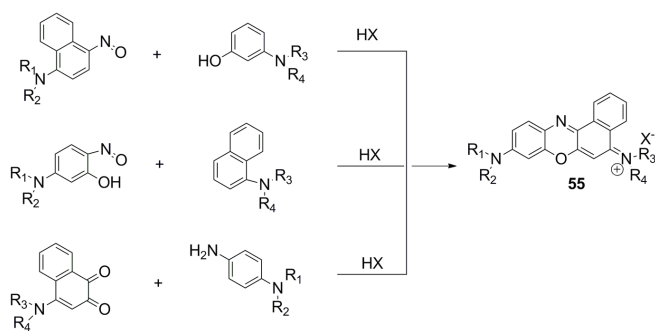
Figure 25. Various synthetic approaches used to obtain oxazine dyes.
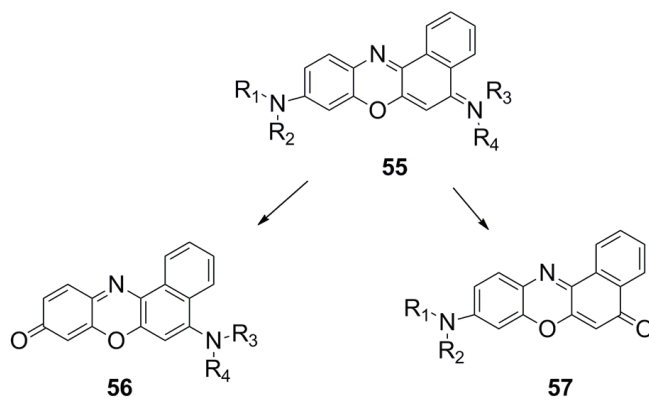
Figure 26. Hydrolysis of an ionic oxazine dye to its non-ionic forms.

acid or in a manner similar to the one shown in **Figure 25** [143]. The stability of the dye, however, is not ideal due to the fact that compound 55 is easily hydrolyzed to the non-ionic naphthoxazinones 56 and 57 (**Figure 26**). Current trends in the development of this family of dyes focuses on the stabilization of the dye by designing rigid ring systems on the terminal amine. According to Sauer *et al*, a bridged amine also promotes facile attachment of a functional group, which can be used for future conjugation with analytes. Regarding this innovative synthesis, Kanitz *et al* reported a very efficient approach for the preparation of bridged naphthoxazinium salts [143].

Near-infrared features and dye quantum yields

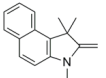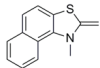According to molecular orbital theory, at longer absorption wavelengths fluorescence efficiency tends to decrease with a decreasing energy difference between the S_1 and S_0 energy levels, especially for hydrogen vibrations. This leads to a decreased quantum yield in the NIR region via internal conversion between S_1 and S_0. Unfortunately, this intrinsic property contributes largely to the low quantum yield in most NIR dyes. In addition, environmental factors such as aggregation, twisting of the heterocyclic rings (i.e. cyanine dyes) or the N-H bond vibrations present in the NH_2 moiety on rhodamine dyes also contribute to the decrease in quantum yield efficiency. One way to improve the quantum yield, in respect to aggregation, can be achieved by the incorporation of sulfonyl groups which tend to lower the occurrence of aggregation [144]. Another strategy used to avoid aggregation, particularly for the cyanine family of dyes, is the use of polymethine bridges. As **Figure 27** shows, for every double bond increase in the methine bridge there is an observable shift of roughly 100 nanometers toward the red region compared to 20 nanometers of the same shift for each additional aromatic ring. This suggests that aggregation is not occurring with each addition of a methine group into the backbone. In rhodamine dyes, replacing the NH_2 with NR_2 and making the ring system more rigid also leads to a dramatic increase in fluorescence with the quantum yield efficiency significantly improved.

Fluorescence resonance energy transfer (FRET)

Fluorescence Resonance Energy Transfer (FRET) is a hallmark of fluorescence technology and thus it is worth mentioning in this optical probe section. As a matter a fact, FRET has been employed for generating "smart" activated protease sensing probes [118]. This technique has been used widely dealing with problems on the scale of molecular distance, proximities, orientations and dynamic properties [145]. The process is characterized by the transfer of extra electronic excitation energy from a donor chromophore to an acceptor molecule brought in close proximity via a through-space dipole-dipole coupling mechanism between the donor-acceptor pair. The efficiency of the transfer process is dependent on the inverse sixth power of the distance between the fluorophores,

Ring system	Bridge Length (n)	λ_{abs}	λ_{em}
	1	490	515
	2	585	620
	3	680	740
	1	550	590
	2	650	690
	3	750	790
	1	570	610
	2	680	720
	3	795	835
	1	560	590
	2	660	690
	3	765	810
	1	600	630
	2	700	740
	3	815	855

Figure 27. Comparison between the number of methine linkers and the resulting maximum absorption and emission wavelengths (l).

meaning that the smaller the distance, the greater the efficiency. Distances as great as 70Å have displayed an adequate level of donor to acceptor excitation energy transfer [146].

The advent of optical devices, especially the charge-coupled device (CCD) camera, and computer-based imaging technology has afforded a forthright way to detect dequenching photons from FRET activation *in vivo*. As a result, the FRET technique takes center stage in the optical imaging of molecular events such as protease-associated biochemical pathways [118]. However, it is noteworthy to mention that there are limitations in FRET measurements, particularly with high substrate concentrations where the fluorescence intensities are not proportional to the concentration of activated products. This leads to an underestimation of the fluorescent signal from the donor chromophore. This phenomenon may result when the fluorescent compound can be re-absorbed by acceptor groups on neighboring substrates or by contamination resulting from the cleavage of the FRET molecules [147].

The use of FRET, in conjunction with the development of specifically targeted molecular

probes, not only enhances signal contrast, but also enables the imaging of specific molecular events associated with the disease state. Methods for the development of specific peptide-based activatable molecular beacons for the detection of protease activity using Förster Resonance Energy Heterotransfer (FREHT) have previously been reported. These probes can be synthesized using commercially available Cy5.5 and previously developed NIR dyes as both donors and acceptors. Conjugation of the FREHT compound to a suitable peptide containing a sequence specifically designed for recognition and cleavage by proteases allows for the detection of protease activity. This construct underscored the development of highly stable red-shifted acceptor dyes that met the criteria outlined above and could be directly conjugated onto a peptide [118].

Molecular beacons that use FRET technology to monitor fluorescent signals have also been widely used in the detection of nucleotides [148-155]. In general, the system consists of a hairpin-forming DNA strand labeled on the ends with a fluorochrome (donator) and a silencer (acceptor) with the spatial distance between the fluorochrome and the silencer large enough to show a large fluorescent signal when the DNA strand is interacting with its complementary sequence. When the DNA is not interacting with the complimentary sequence, it undergoes hairpin formation, which brings the fluorochrome and silencer into close proximity causing a decrease in fluorescent signal. In order to gain a dramatic change in fluorescent signals, Kool *et al* developed a module where the silencer, Dabcyl, acts as a leaving group upon the joining of two DNA strands. After the oligonucleotide had been modified with the silencer Dabcyl and fluorescein, a 99% quenching efficiency was observed. The Dabcyl was cleaved upon ligation of the two DNA strands on a complementary DNA template. Remarkably, this probe could detect a single point of mutation on a target DNA [156].

Chemistry of MRI probes

Introduction to MRI

MRI has become one of the most reliable diagnostic imaging modalities, coupling high spatial resolution with exquisite dynamic information and anatomical contrast. Similar to nuclear magnetic resonance (NMR), MRI relies on the
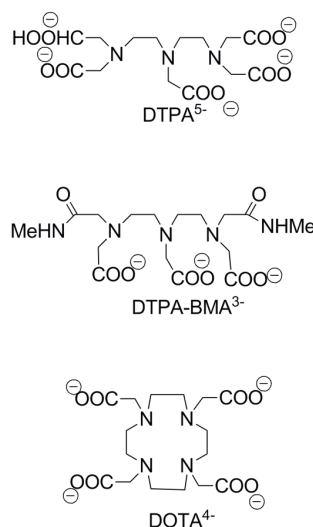
relaxation efficiency of protons (in this case water protons) placed in a fixed magnetic field. The contrast obtained in images is commonly due to different relaxation rates of protons found in different tissues. Contrast enhancement can be achieved via the use of so-called contrast agents, which have the ability to shorten either T_1 or T_2 relaxation times. Contrast agents include, but are not limited to, paramagnetic ions such as gadolinium (Gd^{3+}) and other lanthanide ions, which are T_1 agents and ferromagnetic iron oxide particles and nanoparticles, which are T_2 agents. Gadolinium contrast agents are by far the most popular choice of contrast agent, with greater than 10 million MRI studies done each year [157, 158].

Gadolinium and related lanthanide contrast agents

Free gadolinium ion has been found to have a biological half-life on the order of several weeks with a primary mechanism of excretion through the kidneys and liver, implying that the administering and evaluation of free gadolinium ion would be sufficiently long lived to obtain high quality images. Unfortunately, free gadolinium has also been found to have a high toxicity profile [159]. In order to reduce the toxic nature of the free ion, it has been deemed necessary to encapsulate the ion in a multidentate chelate enabling the effective sequestering of the ion from biological processes. Common examples of the necessary octadentate chelates, shown in **Figure 28**, include diethylene triamine pentaacetic acid (DPTA), 5,8-bis(carboxymethyl)-11-[2-(methylamino)-2-oxoethyl]-3-oxo-2,5,8,11-tetraazatridecan-13-oic acid (DTPA-BMA) and 1,4,7,10-tetraazacyclododecane-N, N', N'', N'''-tetraacetic acid (DOTA). These chelates have been found to be sufficiently bulky to prevent a rapid release of the ion, but not so bulky as to not allow for the necessary water interactions with the paramagnetic gadolinium center [160].
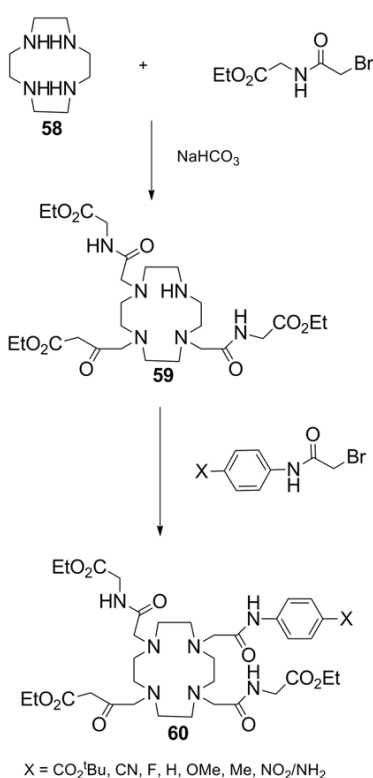
The ability of gadolinium complexes to shorten the observed T_1 has been attributed to two separate modes of water relaxation; termed *inner sphere* and *outer sphere*. *Inner sphere* refers to the relaxation occurring due to the co-ordination between water molecules and the metal center. This coordination is by no means a permanent interaction and actually relies on the rapid exchange of water molecules at a rate shorter than T_1, but long enough to ensure adequate relaxation. *Outer sphere* refers to the relaxation due to water molecules dynamically diffusing near the paramagnetic metal centers and experiencing fluctuations in the local magnetic field [161].

Figure 28. A sampling of the common chelates that have been used to lower the toxicity of gadolinium ions.

In addition to the already discussed water relaxation contrast approach, an alternative type of contrast agent stems from the transfer of selectively saturated spins from one chemical pool to another. This is known as chemical exchange saturation transfer (CEST) and when done in the presence of a paramagnetic agent, such as a lanthanide, this is often referred to as PARACEST [162, 163]. The signal enhancement in PARACEST agents comes from a decrease in signal intensity of bulk water when the protons coordinated to a suitable lanthanide, other than gadolinium, are irradiated. In order for PARACEST to be effective, the rate of water exchange has to be sufficiently slow. Factors that have been found to affect the exchange rate include steric crowding of the coordinating ligand, overall size of the lanthanide ion, coordination geometry adopted by the ligand, quantity of the contrast agent present at the area of interest and the electronic properties of the coordinating ligand [164-167]. Recently, studies were performed to determine the extent to which variations in ligand electronic structures would affect the rate of water exchange. Ratnaker and co-workers synthesized a series of

Figure 29. Synthesis of europium(III) DOTA-tetramide complexes.

Figure 30. Synthetic route used to obtain a 1,7-substituted tetraazamacrocycle for the detection of glucose by MRI.

DOTA-tetraamide complexes **60** with a variety of different electronic modifications on a single arm of the chelate, as shown in **Figure 29** [168]. In this study, it was clearly demonstrated that the seemingly small changes made to a remote functionality produced either a dramatic enhancement in water retention, as was the case when using electron withdrawing groups, or an increase in water exchange, when electron donating groups were used. This leads to the possibility of tailoring chelating systems to obtain the desired amount of water exchange, which would produce the optimum amount of PARACEST signal enhancement.

An alternative approach for the retarding of water exchange involves the use of a biological blocking agent. In one prime example of this approach, it was found that the placement of two arylboronic acids onto the cyclam chelating backbone would act as an effective capture agent for glucose. The capture of glucose, which locks the water molecule in place, not only increases the contrast ability of the PARACEST contrast agent, but gives a reliable method for the quantification of glucose from tissue to tissue [169]. Synthesis of the chelate was accomplished using a regio-specific protection/deprotection approach specifically developed to produce the desired 1,7- and 1,4-substituted tetraazamacrocycles 64 and 68, respectively (**Figures 30** and **31**) [170, 171]. Results showed that the desired PARACEST signal does indeed increase as a function of increasing glucose concentration, with the 1,7-substituted showing the greatest affinity for glucose [172].

Along the same lines as the previous example, Que and co-workers developed a gadolinium based contrast agent that is essentially "turned off" until in the presence of copper, at which point it "turns on" [173]. This is accomplished by synthesizing a mono-substituted cyclam; where the single substituent contains both a pyridine ring and a pendant tridentate ligand. In the absence of copper the pyridine ring acts as a ligand for the gadolinium ion. However, once

Figure 31. Synthetic scheme used for the synthesis of 1,4-substituted tetraazamacrocyles, which were employed for the detection of glucose.

Figure 32. Schematic showing how, in the presence of copper, the contrast agent "turns on" and allows the flow of water into the inner sphere, thereby increasing contrast.

variety of physiological events to induce the polymerization of the gadolinium based contrast agents. This increases the local concentration of the contrast agent, which in turn increases the contrast [174, 175]. Oxidatively susceptible polymeric gadolinium contrast agents have also been developed as a means to increase bodily excretion of the agent. In order to achieve an increased clearance rate, the polymers were designed and synthesized with disulfide bonds present in each gadolinium chelating monomeric unit. Exposure of the disulfide bond to endogenous thiols, such as cysteine and glutathione, induces cleavage, which in turn, produces small molecular 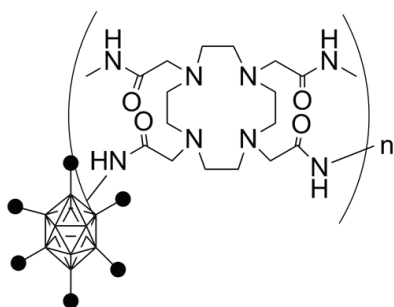gadolinium complexes and oligomers that can be easily eliminated via renal filtration [176]. Results show that the contrast agent is cleared, but this has only been demonstrated in rodents, which have greater plasma thiol concentrations and therefore do not give an accurate comparison of human plasma kinetics.

The use of viral particles for the purpose of directed drug delivery is a concept that has been employed in a variety of studies [177, 178]. Recently, Vasalatiy and coworkers harnessed the power of viral particles in an effort to produce targeted PARACEST contrast agents [179]. The approach explored was synonymous to an approach used in a previous example of this type of directed contrast agent synthesis, which was to use the inherent functionality found on the surface of the particle to attach the contrast agent (**Figure 33**) [180]. Surface functionalization has been shown not to have a detrimental effect on the receptor binding ability of the viral particle [181]. However, this study found that increasing the number of attached ligands decreased the bioactivity of the viral particle, with fewer than ~800 being the optimal number. In addition, it was found that the ligand had to be preloaded

the ligand is exposed to copper it switches roles and becomes a ligand for the copper ion (**Figure 32**). The movement of the pyridine away from the gadolinium center allows for the rapid exchange of bulk water, thereby producing high contrast.

As has already been discussed, targeting of biological entities, such as copper and glucose, is a method that holds great potential for achieving contrast enhancement. However, detection of these species points to the underlying biological processes not necessarily the events themselves. In an effort to accomplish this, many researchers have started to build contrast agents that have been specifically designed to target individual processes or events. One such approach uses the oxidizing ability present in a

Figure 33. Chelate functionalized viral particle.

Figure 34. Simple schematic diagram of a nanoparticle with the various components labeled.

with the lanthanide ion prior to attachment to the particle. If this was not done, non-specific binding of the lanthanide to the chelating agent was observed.

In a different approach, MR imaging of thrombus within fissures of vulnerable atherosclerotic plaques has been attempted using a variety of contrast agents. The types of agents used include peptides and nanoparticles, which will be discussed in the next section. Fibrin, a major constituent of arterial and venous clots, has been one of the predominant targets for the development of peptide contrast agents. These fibrin-specific MRI contrast agents include, but are not limited to; EP-782, EP-821, EP-1084, EP-1086, EP-1873, and EP-2104R [182-184]. Studies have demonstrated that all of these agents, with the exception of EP-821, show statistically significant increases in relaxivity in the presence of fibrin when compared to their relaxivity in buffer. This points to strong fibrin binding causing a receptor induced magnetization enhancement. The lone exception to this is EP-821, which was specifically designed without the necessary fibrin binding, seven amino acid cyclic core (GDYYGTC), in order to serve as a control agent. All studies have thus far only demonstrated the feasibility of using these agents and have not begun full-scale human trials.

Nanoparticles and related contrast agents

The design and synthesis of nanoparticle imaging agents requires very careful consideration in the properties of the particle that are needed or desired in order to target the desired physiological function. A general diagram of a nanoparticle is shown in **Figure 34**. The core can be made of an ever-increasing variety of molecular spe-

cies, such as iron oxide, silica, gold, quantum dots or complex polymers [185]. Contrast can be generated from the core itself, as is the case with iron oxide, or the core can simply act as a means for other contrast agents to be shuttled into the area of interest. In most cases, a biocompatible coating must be added to the surface of the particle in order to allow for a sufficiently long biological half-life. These coatings usually have a large number of functional groups, which allow for ease of functionalization onto the surface. Even with biocompatible species, it has been found that the use of biocompatible compounds such as polymers, need to be attached to the surface of the coating in order to increase the effectiveness of the agent. The last component of a nanoparticle is the targeting agent or contrast agent. These are either small molecules that will direct the particle towards the event of interest or the actual contrast agent, both are attached to the surface of the particle via a suitable linker [186].

In theory, researchers should be able to manipulate all aspects of the four different components that make up the nanoparticles, i.e. the components shown in **Figure 34**, in order to achieve the desired tissue or event specificity they wish to obtain. In an effort to prove this principle a library of nanoparticles were designed and synthesized with both the core and coating held constant, while varying the small molecule directing groups present on the surface [187]. It was found that small molecule
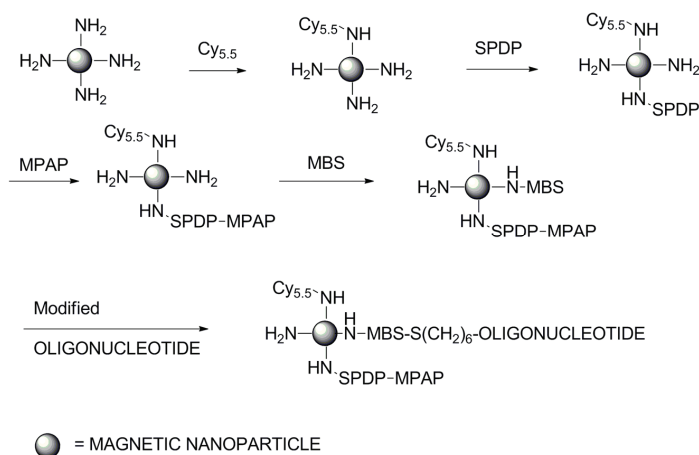
Figure 35. Synthesis of a NIR/MRI iron oxide nanoparticle via a sequential conjugation strategy.

modifications on the surface can modulate the nanoparticle affinity for different cell types and molecular modifications can discriminate between related functional states of cells. This finding provides researchers the potential to develop nanoparticles that are capable of efficiently targeting a desired cell type and therefore increase contrast for that cell type.

As has already been mentioned, a large variety of materials can be used as the core for nanoparticle imaging agents. Magnetic iron oxide has clearly emerged as the core of choice for a variety of biomedical applications for both *in vitro* and *in vivo* imaging [188]. One reason for using this material, especially for tumor imaging, is a proven accumulation of the magnetic nanoparticles within tumors. This accumulation has been attributed to hyperpermeable tumor vasculature resulting from increased cell proliferation [189]. This aspect was used to the advantage of Medarova and co-workers who successfully synthesized a bimodal NIR/MRI iron oxide nanoparticle functionalized with synthetic siRNA molecules designed to target GFP-expressing tumors [190]. The synthesis, shown in **Figure 35**, began with dextran-coated iron oxide nanoparticles, which were first functionalized with Cy5.5 followed by attachment of a heterobifunctional cross-linker, N-succinimidyl 3-(2-pyridyldithio) propionate (SPDP) [191]. Next, myristoylated polyarginine peptide (MPAP) was attached to the SPDP followed by attachment of *m*-maleimidobenzoyl-N-hydroxysuccinimide ester (MBS) crosslinker directly to the nanoparticle

amine. Addition of the MBS allowed for efficient attachment of the desired oligonucleotide providing the final multi-modal imaging agent with an average of three Cy5.5, four MPAP and five siRNA molecules per nanoparticle. Results from this study showed that the agent gave both a favorable biodistribution and excellent imaging characteristics with high resolution, good depth penetration and high sensitivity.

A more chemically simplistic magnetic iron oxide comes in the form of ultrasmall superparamagnetic iron oxide (USPIO). Typical iron oxide particles have a diameter in the range of 30-1,000 nm, USPIO particles are in the range of 5-10 nm [192]. The smaller size allows for a longer blood half-life and gives the particles the ability to transmigrate capillary walls via vesicular transport and interendothelial junctions. For these reasons, USPIO particles have been demonstrated to be effective in the imaging of lymph nodes, atherosclerotic plaque and carotid plaque inflammation [193-195].

As mentioned in the previous section, imaging of thrombus within fissures of vulnerable atherosclerotic plaques has been attempted with a variety of different imaging agents. An example that falls into the class of the functionalized nanoparticle imaging agents is the so-called lipid-encapsulated liquid perfluorocarbon nanoparticle. This class of nanoparticle, possessing no inherent magnetic susceptibility, gains its MRI contrasting ability through the attachment of lanthanide chelating agents directly to the surface. This has been accomplished with both gadolinium chelates and PARACEST chelating agents, such as europium DOTA complexes [196-198]. Both types of imaging agents show high levels of contrast, presumably due to the high level of functionalization on the surface. It was found that greater than 50,000 gadolinium atoms could be appended to the surface of each individual particle, allowing for a large amount of contrast enhancement per particle.

The last categories of nanoparticle that will be mentioned are those with a dendrimer core. Dendrimers are a class of polymers that are grown out from a central molecule by adding additional monomer molecules in a sequential

manner. Each new addition of the monomer can be accomplished in an efficient manner, producing a new "generation" with each subsequent addition. In the case of poly(amidoamine) (PAMAM) dendrimers, each generation theoretically doubles the number of available functional groups on the dendrimer surface. Due to their high ability to be functionalized and the fact that they are nontoxic, makes these types of dendrimers ideal for the development of drug delivery or imaging agents [199]. For an excellent review on the use of dendrimers in medical technology please see Barrett *et Al* [200].

Concluding remarks and perspectives

In today's post-genomic era and in conjunction with novel proteomic techniques, numerous novel biological targets have been idendified, and thus there is great demand for imaging probes that will either help researchers visualize biological targets or screen new drugs. This increased demand offers opportunities as well as challenges to imaging chemists who never before have felt the need for a major overhaul of the synthesis strategies to cope with this new reality. One such revised approach would be to focus on improving reaction maneuvers and accelerating the purification process both of which have far-reaching effects in modern imaging chemistry laboratories. In recent years, for example, we have witnessed the integration of diverse and robust automated systems such as microwave-assisted synthesizers, microfluidic PET labeling modules and photodiode array-equipped flash chromatograpy. Thanks to these advances, overall reaction time has been reduced dramatically and the scales of the reactions are becoming smaller and increasingly more accurate. As a result, these revised approaches can now be adapted for use in high-throughput syntheses of molecular imaging agents. However, regardless of whether these agents are MRI contrast, PET, optical or a combination of any of these modalities, there is a constant need for skilled chemists capable of producing such agents at both the tracer levels as well as in larger scale preparations.

Another contemporary approach focuses on the development of labeling kits or activated linkers that enable non-chemists to partcipate in the end-point process. Specifically, linkers used to label unstable macromolecules such as antibodies and proteins with NIR dyes have proven

useful. Notably, several applications have already benefited from this family of functionalized linkers since the bioconjugation experiments are robust and relatively simple. A pronounced shortfall still exists in this area, however, for example, a PET ready-to-label kit similar to those available for optical probe preparation has yet to be developed. Even from an optimistic perspective, an enormous amount of work must be accomplished before this can become a reality.

If efforts to synthesize versatile PET labeling kits are successful, the result could change the entire PET chemistry landscape. Not only would such an approach correspond favorably with today's predilection for diversity, but it would eventually lead to obviating the need for expensive PET chemistry facilities and their laboratory staffs. Since PET chemistry remains a bottleneck step in most clinical research entities, this initiative merits further investigation from across the molecular imaging spectrum.

Acknowledgement

Address correspondence to: Dr. Wellington Pham, Vanderbilt University, Institute of Imaging Science, Department of Radiology, 1161 21st Avenue South, Nashville, TN 37232-2310 Tel: (615) 936-7621; Fax: (615) 322-0734; E-mail: wellington.pham@vanderbilt.edu

References

[1] Condeelis J and Weissleder R. In vivo imaging in cancer. Cold Spring Harb Perspect Biol 2010; 2: a003848.
[2] New SE and Aikawa E. Molecular imaging insights into early inflammatory stages of arterial and aortic valve calcification. Circ Res 2011; 108: 1381-1391.
[3] Raymond SB, Skoch J, Hills ID, Nesterov EE, Swager TM and Bacskai BJ. Smart optical probes for near-infrared fluorescence imaging of Alzheimer's disease pathology. Eur J Nucl Med Mol Imaging 2008; 35 Suppl 1: S93-98.
[4] Reynolds F and Kelly KA. Techniques for Molecular Imaging Probe Design. Mol Imaging 2011.
[5] Kelloff GJ, Krohn KA, Larson SM, Weissleder R, Mankoff DA, Hoffman JM, Link JM, Guyton KZ, Eckelman WC, Scher HI, O'Shaughnessy J, Cheson BD, Sigman CC, Tatum JL, Mills GQ, Sullivan DC and Woodcock J. The progress and

promise of molecular imaging probes in on-cologic drug development. Clin Cancer Res 2005; 11: 7967-7985.

[6] Bogdanov A Jr and Mazzanti ML. Molecular magnetic resonance contrast agents for the detection of cancer: past and present. Semin Oncol 2011; 38: 42-54.

[7] Lee JS, Vendrell M and Chang YT. Diversity-oriented optical imaging probe development. Curr Opin Chem Biol 2011; 15: 760-767.

[8] Luo S, Zhang E, Su Y, Cheng T and Shi C. A review of NIR dyes in cancer targeting and imaging. Biomaterials 2011; 32: 7127-7138.

[9] Nagano T. Development of fluorescent probes for bioimaging applications. Proc Jpn Acad Ser B Phys Biol Sci 2010; 86: 837-847.

[10] Swierczewska M, Lee S and Chen X. The design and application of fluorophore-gold nanoparticle activatable probes. Phys Chem Chem Phys 2011; 13: 9929-9941.

[11] Phelps ME. positron emission tomography provides molecular imaging of biological processes. Proc Natl Acad Sci USA 2000; 97: 9226-9233.

[12] Brady F, Luthra SK, Brown GD, Osman S, Aboagye E, Saleem A and Price PM. Radiolabelled tracers and anticancer drugs for assessment of therapeutic efficacy using PET. Curr Pharm Des 2001; 7: 1863-1892.

[13] Mandelkern MA. Nuclear techniques for medical imaging: positron emission tomography. Annu Rev Nucl Part Sci 1995; 45: 205-254.

[14] Jalilian AR, Tabatabai SA, Shafiee A, Afarideh H, Najafi R and Bineshmarvasti M. One-step, no-carrier-added, synthesis of a 18F-labeled benzodiazepine receptor ligand. J Labelled Compd Rad 2000; 43: 545-555.

[15] Mueller K, Faeh C and Diederich F. Fluorine in Pharmaceuticals: Looking Beyond Intuition. Science (Washington, DC, United States) 2007; 317: 1881-1886.

[16] Le Bars D. Fluorine-18 and medical imaging: Radiopharmaceuticals for positron emission tomography. J Fluorine Chem 2006; 127: 1488-1493.

[17] Moon BS, Park JH, Lee HJ, Kim JS, Kil HS, Lee BS, Chi DY, Lee BC, Kim YK and Kim SE. Highly efficient production of [18F]fallypride using small amounts of base concentration. Appl Radiat Isotopes 2010; 68: 2279-2284.

[18] Makosza M, Jagusztyn-Grochowska M, Ludwikow M and Jawdosiuk M. Reactions or organic anions. I. Reactions of phenylacetonitrile derivatives with aromatic nitro compounds in basic media. Tetrahedron 1974; 30: 3723-3735.

[19] Lee SJ, Oh SJ, Chi DY, Kang SH, Kil HS, Kim JS and Moon DH. One-step high-radiochemical-yield synthesis of [18F]FP-CIT using a protic solvent system. Nucl Med Biol 2007; 34: 345-351.

[20] Kim DW, Ahn DS, Oh YH, Lee S, Kil HS, Oh SJ, Lee SJ, Kim JS, Ryu JS, Moon DH and Chi DY. A New Class of SN2 Reactions Catalyzed by Protic Solvents: Facile Fluorination for Isotopic Labeling of Diagnostic Molecules. J Am Chem Soc 2006; 128: 16394-16397.

[21] Guo N, Alagille D, Tamagnan G, Price RR and Baldwin RM. Microwave-induced nucleophilic [18F]fluorination on aromatic rings: synthesis and effect of halogen on [18F]fluoride substitution of meta-halo (F, Cl, Br, I)-benzonitrile derivatives. Appl Radiat Isotopes 2008; 66: 1396-1402.

[22] Aigbirhio FI, Carr RM, Pike VW, Steel CJ and Sutherland DR. Automated radiosynthesis of no-carrier-added [S-fluoromethyl-18F]fluticasone propionate as a radiotracer for lung deposition studies with PET. J Labelled Compd Rad 1997; 39: 567-584.

[23] Jeong JM, Lee DS, Chung J-K, Lee MC, Koh C-S and Kang SS. Synthesis of no-carrier-added [18F]fluoroacetate. J Labelled Compd Rad 1997; 39: 395-399.

[24] Luo H, Beets AL, McAllister MJ, Greenbaum M, McPherson DW and Knapp FF, Jr. Resolution, in vitro and in vivo evaluation of fluorine-18-labeled isomers of 1-azabicyclo[2.2.2]oct-3-yl-(1-fluoropent-5-yl)-.alpha.-hydroxy-phenylacetate (FQNPe) as new PET candidates for the imaging of muscarinic-cholinergic receptor. J Labelled Compd Rad 1998; 41: 681-704.

[25] Gilissen C, Bormans G, Groot T and Verbruggen A. Synthesis of N-(2-[18F] fluoroethyl)-N'-methylthiourea: a hydrgen peroxide scavenger. J labelled Compd Rad 1998; 41: 661-681.

[26] Evans PH. Free radicals in brain metabolism and pathology. Brit Med Bull 1993; 49: 577-587.

[27] Law MP, Wagner S, Kopka K, Renner C, Pike VW, Schober O and Schaefers M. Preclinical evaluation of an 18F-labelled Œ≤1-adrenoceptor selective radioligand based on ICI 89,406. Nucl Med Biol 2006; 37: 517-526.

[28] Wagner S, Law MP, Riemann B, Pike VW, Breyholz H-J, Hoeltke C, Faust A, Renner C, Schober O, Schaefers M and Kopka K. Synthesis of an 18F-labeled high affinity Œ≤1-adrenoceptor PET radioligand based on ICI 89,406. J Labelled Compd Rad 2006; 49: 177-195.

[29] Le Bars D, Lemaire C, Ginovart N, Plenevaux A, Aerts J, Brihaye C, Hassoun W, Leviel V, Mekhsian P and Weissmann D. High-Yield Radiosynthesis and Preliminary In Vivo Evaluation of p-[18F] MPPF, a Fluoro Analog of WAY-100635. Nucl Med Biol 1998; 25: 343-350.

[30] Fei X, Zheng QH, Wang JQ, Stone KL, Martinez TD, Miller KD, Sledge GW and Hutchins GD. Synthesis, biodistribution and micro-PET imaging of radiolabeled antimitotic agent T138067 analogues. Bioorg Med Chem Lett 2004; 14: 1247-1251.

[31] Willis PG, Pavlova OA, Chefer SI, Vaupel DB, Mukhin AG and Horti AG. Synthesis and struc-

ture-activity relationship of a novel series of aminoalkylindoles with potential for imaging the neuronal cannabinoid receptor by positron emission tomography. J Med Chem 2005; 48: 5813-5822.

[32] Defraiteur C, Lemaire C, Luxen A and Plenevaux A. Radiochemical synthesis and tissue distribution of p-[18F]DMPPF, a new 5-HT1A ligand for PET, in rats. Nucl Med Biol 2006; 33: 667-675.

[33] Gao M, Wang M, Miller KD, Sledge GW, Hutchins GD and Zheng Q-H. Synthesis of radiolabeled stilbene derivatives as new potential PET probes for aryl hydrocarbon receptor in cancers. Bioorg Med Chem Lett 2006; 16: 5767-5772.

[34] Furukawa N, Ogawa S, Kawai T and Oae S. ipso-Substitution of a sulfinyl or sulfonyl group attached to pyridine rings and its application for the synthesis of macrocycles. J Chem Soc Perkin Trans 1984;1:1839-1845.

[35] Bartoli G, Latrofa A, Naso F and Todesco PE. Fluorodenitration of some mildly activated nitro compounds. J Chem Soc Perkin Trans 1 1972; 2671.

[36] Finger GC, Starr LD, Dickerson DR, Gutowsky HS and Hamer J. Aromatic fluorine compounds. XI. Replacement of chlorine by fluorine in halopyridines. J Org Chem 1963; 28: 1666-1668.

[37] Hamer J, Link WJ, Jurjevich A and Vigo TL. Preparation of 2-fluoroquinoline and 2,6-difluoropyridine by halogen exchange. Rec Trav Chim 1962; 81: 1058-1060.

[38] Ding YS, Sugano Y, Koomen J and Aggarwal D. Synthesis of [18F]Ro 41-0960, a potent catechol-O-methyltransferase inhibitor, for PET studies. J Labelled Compd Rad 1997; 39: 303-318.

[39] Ding YS, Shiue CY, Fowler JS, Wolf AP and Plenevaux A. No-Carrier-Added(NCA) aryl [18F] Fluorides Via The Nucleophilic Aromatic Substituition of Electron-Rich aromatic Rings. J Fluorine Chem 1990; 48: 189-205.

[40] Kilbourn MR and Haka MS. Synthesis of [18F] GBR13119, a presynaptic dopamine uptake antagonist. Int J Rad Appl Instrum [A] 1988; 39: 279-282.

[41] Lemaire C, Guillaume M, Christiaens L, Palmer AJ and Cantineau R. A new route for the synthesis of [18F]fluoroaromatic substituted amino acids: no carrier added L-p-[18F] fluorophenylalanine. Appl Radiat Isotopes 1987; 38: 1033-1038.

[42] Angelini G, Speranza M, Wolf AP and Shiue CY. Nucleophilic aromatic substitution of activated cationic groups by fluorine-18-labeled fluoride. A useful route to no-carrier-added (NCA) fluorine-18-labeled aryl fluorides. J Fluorine Chem 1985; 27: 177-191.

[43] Haka MS, Kilbourn MR, Watkins GL and Toorongian SA. Aryltrimethylammonium trifluoromethanesulfonates as precursors to aryl [18F]fluorides: improved synthesis of [18F]

GBR-13119. J Labelled Compd Rad 1989; 27: 823-833.

[44] Fredriksson A, Johnström P, Stone-Elander S, Jonasson P, Nygren P, Ekberg K, Johansson B and Wahren J. Labeling of human C-peptide by conjugation with succinimidyl-4-fluorobenzoate. J Labelled Compd Rad 2001; 44: 509-519.

[45] Ding Y-S. 18F-labeled biomolecules for PET studies in the neurosciences. J Fluorine Chem 2000; 101: 291-295.

[46] Guenther KJ, Yoganathan S, Garofalo R, Kawabata T, Strack T, Labiris R, Dolovich M, Chirakal R and Valliant JF. Synthesis and in Vitro Evaluation of 18F- and 19F-Labeled Insulin: A New Radiotracer for PET-based Molecular Imaging Studies. J Med Chem 2006; 49: 1466-1474.

[47] Berndt M, Pietzsch J and Wuest F. Labeling of low-density lipoproteins using the 18F-labeled thiol-reactive reagent N-[6-(4-[18F] fluorobenzylidene)aminooxyhexyl]maleimide. Nucl Med Biol 2007; 34: 5-15.

[48] Wüst F, Hultsch C, Bergmann R, Johannsen B and Henle T. Radiolabelling of isopeptide N[var epsilon]-(glutamyl)--lysine by conjugation with N-succinimidyl-4-[18F]fluorobenzoate. Appl Radiat Isotopes 2003; 59: 43-48.

[49] Getvoldsen G, Fredriksson A, Elander N and Stone-Elander S. Microwave-assisted cyclocondensation of 1, 2-diaminobenzene with [4-18 F] fluorobenzoic acid: microwave synthesis of 2-([4-18 F] fluorophenyl) benzimidazole. J Labelled Compd Rad 2004; 47: 139-146.

[50] Hultsch C, Berndt M, Bergmann R and Wuest F. Radiolabeling of multimeric neurotensin(8-13) analogs with the short-lived positron emitter fluorine-18. Appl Radiat Isotopes 2007; 65: 818-826.

[51] Schirrmacher R, Bradtmoller G, Schirrmacher E, Thews O, Tillmanns J, Siessmeier T, Buchholz HG, Bartenstein P, Wangler B and Niemeyer CM. 18F-Labeling of Peptides by means of an Organosilicon-Based Fluoride Acceptor. Angew Chem Int Ed 2006; 45: 6047.

[52] Pietzsch J, Bergmann R, Rode K, Hultsch C, Pawelke B, Wuest F and van den Hoff J. Fluorine-18 radiolabeling of low-density lipoproteins: a potential approach for characterization and differentiation of metabolism of native and oxidized low-density lipoproteins in vivo. Nucl Med Biol 2004; 31: 1043-1050.

[53] Wester H-J, Hamacher K and Stöcklin G. A comparative study of N.C.A. Fluorine-18 labeling of proteins via acylation and photochemical conjugation. Nucl Med Biol 1996; 23: 365-372.

[54] Guhlke S, Coenen HH and Stoecklin G. Fluoroacylation agents based on small n.c.a. [18F] fluorocarboxylic acids. Appl Radiat Isotopes 1994; 45: 715-727.

[55] Vaidyanathan G and Zalutsky MR. Improved Synthesis of N-Succinimidyl 4-[18F] Fluorobenzoate and Its Application to the Labeling of a Monoclonal Antibody Fragment. Biocon-

jugate Chem 1994; 5: 352-356.

[56] Shai Y, Kirk KL, Channing MA, Dunn BB, Lesniak MA, Eastman RC, Finn RD, Roth J and Jacobson KA. 18F-labeled insulin: a prosthetic group methodology for incorporation of a positron emitter into peptides and proteins. Biochemistry 1989; 28: 4801-4806.

[57] Kilbourn MR, Dence CS, Welch MJ and Mathias CJ. Fluorine-18 labeling of proteins. J Nucl Med 1987; 28: 462-470.

[58] Wester HJ, Hamacher K and Stocklin G. A comparative study of N.C.A. fluorine-18 labeling of proteins via acylation and photochemical conjugation. Nucl Med Biol 1996; 23: 365-372.

[59] Toyokuni T, Walsh JC, Dominguez A, Phelps ME, Barrio JR, Gambhir SS and Satyamurthy N. Synthesis of a New Heterobifunctional Linker, N-[4-(Aminooxy)butyl]maleimide, for Facile Access to a Thiol-Reactive 18F-Labeling Agent. Bioconjugate Chem 2003; 14: 1253-1259.

[60] Dolci L, Dolle F, Jubeau S, Vaufrey F and Crouzel C. 2-[18F]fluoropyridines by no-carrier-added nucleophilic aromatic substitution with [18F]FK-K222 - a comparative study. J Labelled Compd Rad 1999; 42: 975-985.

[61] Knust EJ, Machulla MJ and Molls M. J labelled compd rad 1982; 19: 1643-1644.

[62] Ballinger JR, Bowen BM, Firnau G, Garnett ES, Heyes MP, Nahmias C and Teare FW. Synthesis and biodistribution of [F-18]2- and [F-18]6-fluoronicotine. Curr. Appl. Radiopharmacol., Proc Int Symp Radiopharmacol 4th 1986; 17-26.

[63] Dolle F, Valette H, Bottlaender M, Hinnen F, Vaufrey F, Guenther I and Crouzel C. Synthesis of 2-[18F]fluoro-3-[2(S)-2-azetidinylmethoxy] pyridine, a highly potent radioligand for in vivo imaging central nicotinic acetylcholine receptors. J Labelled Compd Rad 1998; 41: 451-463.

[64] Liang F, Navarro HA, Abraham P, Kotian P, Ding YS, Fowler J, Volkow N, Kuhar MJ and Carroll Fl. Synthesis and Nicotinic Acetylcholine Receptor Binding Properties of exo-2-(2'-Fluoro-5'-pyridinyl)-7-azabicyclo[2.2.1]heptane: A New Positron Emission Tomography Ligand for Nicotinic Receptors. J Med Chem 1997; 1997: 2293-2295.

[65] Knust EJ, Machulla HJ and Molls MJ. 18-F-Production In A Water Target With High Yields For 18-F-Labelling Of Organic Compounds: Synthesis of 6-(18F)-Nicotinic Acid Diethylamide. J Labelled Compd Rad 1982; 19: 1643.

[66] Ballinger JR, Bowen BM, Firnau G, Stephen Garnett E and Teare FW. Radiofluorination with reactor-produced Cesium [18F]fluoride: No-carrier-added [18F]2-fluoronicotine and [18F]6-fluoronicotine. Int J Appl Radiat Isotopes 1984; 35: 1125-1128.

[67] Dolci L, Dolle F, Valette H, Vaufrey F, Fuseau C, Bottlaender M and Crouzel C. Synthesis of a fluorine-18 labeled derivative of epibatidine for in vivo nicotinic acetylcholine receptor PET imaging. Bioorgan Med Chem 1999; 7: 467-479.

[68] Karramkam M, Hinnen F, Berrehouma M, Hlavacek C, Vaufrey F, Halldin C, McCarron JA, Pike VW and Dollé F. Synthesis of a [6-Pyridinyl-18F]-labelled fluoro derivative of WAY-100635 as a candidate radioligand for brain 5-HT1A receptor imaging with PET. Bioorgan Med Chem 2003; 11: 2769-2782.

[69] Zhang Y, Pavlova OA, Chefer SI, Hall AW, Kurian V, Brown LL, Kimes AS, Mukhin AG and Horti AG. 5-Substituted Derivatives of 6-Halogeno-3-((2-(S)-azetidinyl)methoxy)pyridine and 6-Halogeno-3-((2-(S)-pyrrolidinyl)methoxy)pyridine with Low Picomolar Affinity for 2 Nicotinic Acetylcholine Receptor and Wide Range of Lipophilicity: Potential Probes for Imaging with Positron Emission Tomography. J Med Chem 2004; 47: 2453-2465.

[70] Simeon FG, Wendahl MT and Pike VW. The [18F]2-fluoro-1,3-thiazolyl moiety-an easily-accessible structural motif for prospective molecular imaging radiotracers. Tetrahedron Lett 2010; 51: 6034-6036.

[71] Füchtner F and Steinbach J. Efficient synthesis of the 18F-labelled 3-O-methyl-6-[18F]fluoro-L-DOPA. Appl Radiat Isotopes 2003; 58: 575-578.

[72] VanBrocklin HF, Blagoev M, Hoepping A, O'Neil JP, Klose M, Schubiger PA and Ametamey S. A new precursor for the preparation of 6-[18F] Fluoro--m-tyrosine ([18F]FMT): efficient synthesis and comparison of radiolabeling. Appl Radiat Isotopes 2004; 61: 1289-1294.

[73] Namavari M, Bishop A, Satyamurthy N, Bida G and Barrio JR. Regioselective radiofluorodestannylation with fluorine-18 and [18F] acetyl hypofluorite: a high yield synthesis of 6-[18F] fluoro-L-dopa. Appl Radiat Isotopes 1992; 43: 989-996.

[74] De Vries EFJ, Luurtsema G, Brussermann M, Elsinga PH and Vaalburg W. Fully automated synthesis module for the high yield one-pot preparation of 6-[18F]fluoro-L-DOPA. Appl Radiat Isotopes 1999; 51: 389-394.

[75] Dolle F, Demphel S, Hinnen F, Fournier D, Vaufrey F and Crouzel C. 6-[18F]Fluoro-L-DOPA by radiofluorodestannylation: a short and simple synthesis of a new labeling precursor. J Labelled Compd Rad 1998; 41: 105-114.

[76] Namavari M, Satyamurthy N, Phelps ME and Barrio JR. Synthesis of 6-[18F] and 4-[18F] fluoro-l-m-tyrosines via regioselective radiofluorodestannylation. Appl Radiat Isotopes 1993; 44: 527-536.

[77] Chen DW and Ochiai M. Chromium(II)-Mediated Reactions of Iodonium Tetrafluoroborates with Aldehydes: Umpolung of Reactivity of Diaryl-, Alkenyl(aryl)-, and Alkynyl(aryl)iodonium Tetrafluoroborates. J Org Chem 1999; 64: 6804-6814.

[78] Okuyama T, Takino T, Sueda T and Ochiai M.

Solvolysis of Cyclohexenyliodonium Salt, a New Precursor for the Vinyl Cation: Remarkable Nucleofugality of the Phenyliodonio Group and Evidence for Internal Return from an Intimate Ion-Molecule Pair. J Am Chem Soc 1995; 117: 3360-3367.

[79] Grushin VV, Demkina II and Tolstaya T. Unified mechanistic analysis of polar reactions of diaryliodonium salts. Perkin transactions. 2 1992; 4: 505-511.

[80] Grushin VV. Carboranylhalonium ions: from striking reactivity to a unified mechanistic analysis of polar reactions of diarylhalonium compounds. Accounts Chem Res 1992; 25: 529-536.

[81] Yamada Y and Okawara M. Steric Effect in the Nucleophilic Attack of Bromide Anion on Diaryl- and Aryl-2-thienyliodonium Ions. Bull Chem Soc Jpn 1972; 45: 1860-1863.

[82] Shah A, Pike VW and Widdowson DA. The synthesis of [18 F] fluoroarenes from the reaction of cyclotron-produced [18 F] fluoride ion with diaryliodonium salts. Journal of the Chemical Society, Perkin Transactions 1 1998; 1998: 2043-2046.

[83] Ross TL, Ermert J, Hocke C and Coenen HH. Nucleophilic 18 F-Fluorination of Heteroaromatic Iodonium Salts with No-Carrier-Added [18 F] Fluoride. J Am Chem Soc 2007; 129: 8018-8025.

[84] Scott PJH. Methods for the Incorporation of Carbon-11 To Generate Radiopharmaceuticals for PET Imaging. Angew Chem Int Ed 2009; 48: 6001-6004.

[85] Kihlberg T and Lngstroem B. Biologically active 11C-labeled amides using palladium-mediated reactions with aryl halides and [11C]carbon monoxide. J Org Chem 1999; 64: 9201-9205.

[86] Langstrom B and Lundqvist H. The preparation of 11C-methyl iodide and its use in the synthesis of 11C-methyl-L-methionine. Int J Appl Radiat Isotopes 1976; 27: 357-363.

[87] Marazano C, Maziere M, Berger G and Comar D. Synthesis of methyl iodide-11C and formaldehyde-11C. Int. J Appl Radiat Isotopes 1977; 28: 49-52.

[88] Chakraborty PK, Gildersleeve DL, Jewett DM, Toorongian SA, Kilbourn MR, Schwaiger M and Wieland DM. High yield synthesis of high specific activity R-(-)-[11C]epinephrine for routine PET studies in humans. Nucl Med Biol 1993; 20: 939-944.

[89] Nagren K, Halldin C, Muller L, Swahn C-G and Lehikoinen P. Comparison of [11C]methyl triflate and [11C]methyl iodide in the synthesis of PET radioligands such as [11C].beta.-CIT and [11C].beta.-CFT. Nucl Med Biol 1995; 22: 965-970.

[90] Kihlberg T, Valind S and Laangstroem B. Synthesis of [1-11C], [2-11C], [1-11C](2H3) and [2-11C](2H3) acetate for in vivo studies of myocardium using PET. Nucl Med Biol 1994; 21:

1067-1072.

[91] Lundkvist C, Halldin C, Swahn C-G, Ginovart N and Farde L. Different brain radioactivity curves in a PET study with [11C].beta.-CIT labelled in two different positions. Nucl Med Biol 1999; 26: 343-350.

[92] Kawashima H, Yajima K, Kuge Y, Hashimoto N and Miyake Y. Synthesis of [1-11C]-2-octynoic acid, [1-11C]-2-decynoic acid and [1-11C]-3-(R,S)-methyloctanoic acid as potential markers for PET studies of fatty acid metabolism. J Labelled Compd Rad 1997; 39: 181-193.

[93] Ravert HT, Klecker RW Jr, Collins JM, Mathews WB, Pomper MG, Wahl RL and Dannals RF. Radiosynthesis of [11C]paclitaxel. J Labelled Compd Rad 2002; 45: 471-477.

[94] Colquhoun HM, Thompson DJ, Twigg MV and Editors. Carbonylation. Direct Synthesis of Carbonyl Compounds. New York and London: Plenum Press, 1991.

[95] Gyorkos AC, Stille JK and Hegedus LS. The total synthesis of (±)-epi-jatrophone and (±)-jatrophone using palladium-catalyzed carbonylative coupling of vinyl triflates with vinyl stannanes as the macrocycle-forming step. J Am Chem Soc 1990; 112: 8465-8472.

[96] Murahashi S, Imada Y and Nishimura K. Palladium-catalyzed carbonylation of allylamines. Synthesis of .beta.,.gamma.-unsaturated amides by one-carbon homologation of allylamines. Tetrahedron 1994; 50: 453-464.

[97] Blower PJ, Lewis JS and Zweit J. Copper radionuclides and radiopharmaceuticals in nuclear medicine. Nucl Med Biol 1996; 23: 957-980.

[98] Pham W, Kobukai S, Hotta C and Gore JC. Dendritic cells: therapy and imaging. Expert Opin Biol Ther 2009; 9: 539-564.

[99] Welch MJ, Redvanly CS and Editors. Handbook of Radiopharmaceuticals: Radiochemistry and Applications. 2003.

[100] Zhang H, Moroz Maxim A, Serganova I, Ku T, Huang R, Vider J, Maecke Helmut R, Larson Steven M, Blasberg R and Smith-Jones Peter M. Imaging expression of the human somatostatin receptor subtype-2 reporter gene with 68Ga-DOTATOC. J Nucl Med 2011; 52: 123-131.

[101] Ferreira CL, Lamsa E, Woods M, Duan Y, Fernando P, Bensimon C, Kordos M, Guenther K, Jurek P and Kiefer GE. Evaluation of Bifunctional Chelates for the Development of Gallium-Based Radiopharmaceuticals. Bioconjugate Chem 2010; 21: 531-536.

[102] Hnatowich DJ, Layne WW, Childs RL, Lanteigne D, Davis MA, Griffin TW and Doherty PW. Radioactive labeling of antibody: a simple and efficient method. Science 1983; 220: 613-615.

[103] Franz J, Freeman GM, Barefield EK, Volkert WA, Ehrhardt GJ and Holmes RA. Labeling of antibodies with copper-64 using a conjugate containing a macrocyclic amine chelating agent. Nucl Med Biol 1987; 14: 479-484.

[104] Bass LA, Wang M, Welch MJ and Anderson CJ. In Vivo Transchelation of Copper-64 from TETA-Octreotide to Superoxide Dismutase in Rat Liver. Bioconjugate Chem 2000; 11: 527-532.

[105] Lewis JS, Lewis MR, Srinivasan A, Schmidt MA, Wang J and Anderson CJ. Comparison of Four 64Cu-Labeled Somatostatin Analogs in Vitro and in a Tumor-Bearing Rat Model: Evaluation of New Derivatives for Positron Emission Tomography Imaging and Targeted Radiotherapy. J Med Chem 1999; 42: 1341-1347.

[106] Wu AM, Yazaki PJ, Tsai S-W, Nguyen K, Anderson A-L, McCarthy DW, Welch MJ, Shively JE, Williams LE, Raubitschek AA, Wong JYC, Toyokuni T, Phelps ME and Gambhir SS. High-resolution microPET imaging of carcinoembryonic antigen-positive xenografts by using a copper-64-labeled engineered antibody fragment. Proc Natl Acad Sci USA 2000; 97: 8495-8500.

[107] Boswell CA, Sun X, Niu W, Weisman GR, Wong EH, Rheingold AL and Anderson CJ. Comparative in Vivo Stability of Copper-64-Labeled Cross-Bridged and Conventional Tetraazamacrocyclic Complexes. J Med Chem 2004; 47: 1465-1474.

[108] Achilefu S, Dorshow RB, Bugaj JE and Rajagopalan R. Novel receptor-targeted fluorescent contrast agents for in vivo tumor imaging. Invest Radiol 2000; 35: 479-485.

[109] Becker A, Hessenius C, Licha K, Ebert B, Sukowski U, Semmler W, Wiedenmann B and Grotzinger C. Receptor-targeted optical imaging of tumors with near-infrared fluorescent ligands. Nat Biotechnol 2001; 19: 327-331.

[110] Licha K, Hessenius C, Becker A, Henklein P, Bauer M, Wisniewski S, Wiedenmann B and Semmler W. Synthesis, characterization, and biological properties of cyanine-labeled somatostatin analogues as receptor-targeted fluorescent probes. Bioconjugate Chem 2001; 12: 44-50.

[111] Zaheer A, Lenkinski RE, Mahmood A, Jones AG, Cantley LC and Frangioni JV. In vivo near-infrared fluorescence imaging of osteoblastic activity. Nat Biotechnol 2001; 19: 1148-1154.

[112] Bremer C, Bredow S, Mahmood U, Weissleder R and Tung CH. Optical imaging of matrix metalloproteinase-2 activity in tumors: feasibility study in a mouse model. Radiology 2001; 221: 523-529.

[113] Marten K, Bremer C, Khazaie K, Sameni M, Sloane B, Tung CH and Weissleder R. Detection of Dysplastic Intestinal Adenomas Using Enzyme-Sensing Molecular Beacons in Mice. Gastroenterology 2002; 122: 406-414.

[114] Tung C-H, Bredow S, Mahmood U and Weissleder R. Preparation of a Cathepsin D Sensitive Near-Infrared Fluorescence Probe for Imaging. Bioconjugate Chem 1999; 10: 892-896.

[115] Tung CH, Mahmood U, Bredow S and Weissleder R. In vivo imaging of proteolytic

[116] Weissleder R, Tung C-H, Mahmood U and Bogdanov A, Jr. In vivo imaging of tumors with protease-activated near-infrared fluorescent probes. Nat Biotechnol 1999; 17: 375-378.

[117] Pham W, Weissleder R and Tung CH. An Azulene Dimer as a Near-Infrared Quencher. Angew Chem Int Ed 2002; 41: 3659-3662.

[118] Pham W, Choi Y, Weissleder R and Tung CH. Developing a peptide-based near-infrared molecular probe for protease sensing. Bioconjugate Chem 2004; 15: 1403-1407.

[119] Weissleder R and Mahmood U. Molecular imaging. Radiology 2001; 219: 316-333.

[120] Brooker LGS and Keyes GH. Cyanine dye series. III. Improvements in the 2'-cyanine condensation. J Am Chem Soc 1935; 57: 2488-2492.

[121] Ficken GE. Cyanine dyes. Chem Syn Dyes 1971; 4: 211-340.

[122] Sturmer DM. Syntheses and properties of cyanine and related dyes. Chem Heterocycl Compd 1977; 30: 441-587.

[123] Tilak BD. Recent developments in synthetic dyes. J Sci Ind Res 1966; 25: 489-493.

[124] Uspenskaya AY and Shapiro BI. J-aggregation of cyanine dyes in photographic layers. Zhurnal Nauchnoi i Prikladnoi Fotografii 2000; 45: 46-75.

[125] Konig W. Chemistry of the quinocyanines. Constitution of the pinacyanoles. Ber Dtsch Chem Ges B 1922; 55B: 3293-3313.

[126] Pham W, Weissleder R and Tung C-H. An azulene dimer as a near-infrared quencher. Angew Chem Int Ed 2002; 41: 3659-3662.

[127] Arai S, Yamazaki M, Nagakura K, Ishikawa M and Hida M. New solvatochromic cyanine dyes derived from 2-methylbenzo[a]quinolizinium perchlorate. J Chem Soc Chem Commun 1983; 1037-1038.

[128] Mujumdar RB, Ernst LA, Mujumdar SR, Lewis CJ and Waggoner AS. Cyanine dye labeling reagents: sulfoindocyanine succinimidyl esters. Bioconjugate Chem 1993; 4: 105-111.

[129] Isacsson J and Westman G. Solid-phase synthesis of asymmetric cyanine dyes. Tetrahedron Lett 2001; 42: 3207-3210.

[130] Konig W. Ber. Dtsch Chem Ges 1922; 55: 3293.

[131] Wang L, Peng X, Zhang R, Cui J, Xu G and Wang F. Syntheses and spectral properties of fluorescent trimethine sulfo-3H-indocyanine dyes. Dyes Pigm 2002; 54: 107-111.

[132] Kovalska VB, Volkova KD, Losytskyy MY, Tolmachev OI, Balanda AO and Yarmoluk SM. 6,6'-Disubstituted benzothiazole trimethine cyanines - new fluorescent dyes for DNA detection. Spectrochim Acta, Part A 2006; 65A: 271-277.

[133] Benson RC and Kues HA. Absorption and fluorescence properties of cyanine dyes. J Chem Eng Data 1977; 22: 379-383.

[134] Konig W. "Vinylene-homologous" indole and

pyrrole dyes. Angew Chem 1925; 38: 743-748.

[135] Ernst LA, Gupta RK, Mujumdar RB and Waggoner AS. Cyanine dye labeling reagents for sulfhydryl groups. Cytometry 1989; 10: 3-10.

[136] Randolph JB and Waggoner AS. Stability, specificity and fluorescence brightness of multiply-labeled fluorescent DNA probes. Nucleic Acids Res 1997; 25: 2923-2929.

[137] Reynolds GA and Drexhage KH. Stable heptamethine pyrylium dyes that absorb in the infrared. J Org Chem 1977; 42: 885-888.

[138] Tyutyulkov N, Fabian J, Mehlhorn A, Dietz F and Tadjer A. Polymethine Dyes: Structure and Properties. 1991.

[139] Lefevre C, Kang HC, Haugland RP, Malekzadeh N, Arttamangkul S and Haugland RP. Texas Red-X and Rhodamine Red-X, New Derivatives of Sulforhodamine 101 and Lissamine Rhodamine B with Improved Labeling and Fluorescence Properties. Bioconjugate Chem 1996; 7: 482-489.

[140] Leytus SP, Patterson WL and Mangel WF. New class of sensitive and selective fluorogenic substrates for serine proteinases. Amino acid and dipeptide derivatives of rhodamine. Biochem J 1983; 215: 253-260.

[141] Peters U, Falk LC and Kalman SM. Digoxin metabolism in patients. Arch Intern Med 1978; 138: 1074-1076.

[142] Lam JY, Benson SC and Menchen SM. Extended Rhodamine Compounds Useful As Fluorescent Lables. US 6,248,884 B1 2001; 37.

[143] Kanitz A and Hartmann H. Preparation and characterization of bridged naphthoxazinium salts. European J Org Chem 1999; 923-930.

[144] Becker A, Hessenius C, Bhargava S, Grotzinger C, Licha K, Schneider-Mergener J, Wiedenmann B and Semmler W. Cyanine dye labeled vasoactive intestinal peptide and somatostatin analog for optical detection of gastroenteropancreatic tumors. Ann N Y Acad Sci 2000; 921: 275-278.

[145] Clegg RM. FRET tells us about proximities, distances, orientations and dynamic properties. Rev Mol Biotechnol 2002; 82: 177-179.

[146] Stryer L. Fluorescence energy transfer as a spectroscopic ruler. Annu Rev Biochem 1978; 47: 819-846.

[147] Albrecht C. Principles of fluorescence spectroscopy, 3rd Edition, Joseph R. Lakowicz, editor. Springer : New York, 2008.

[148] Antony T and Subramaniam V. Molecular beacons: nucleic acid hybridization and emerging applications. J Biomol Struct Dyn 2001; 19: 497-504.

[149] Fang X, Li JJ and Tan W. Using Molecular Beacons To Probe Molecular Interactions between Lactate Dehydrogenase and Single-Stranded DNA. Anal Chem 2000; 72: 3280-3285.

[150] Heyduk T and Heyduk E. Molecular beacons for detecting DNA binding proteins. Nat Biotechnol 2002; 20: 171-176.

[151] Jovine L. Molecular beacons meet DNA-protein interactions: bye bye bandshift? Trends Biotechnol 2002; 20: 190.

[152] Kuhn H, Demidov VV, Coull JM, Fiandaca MJ, Gildea BD and Frank-Kamenetskii MD. Hybridization of DNA and PNA molecular beacons to single-stranded and double-stranded DNA targets. J Am Chem Soc 2002; 124: 1097-1103.

[153] Liu J, Feldman P and Chung TDY. Real-Time Monitoring in Vitro Transcription Using Molecular Beacons. Anal Biochem 2002; 300: 40-45.

[154] Tyagi S and Kramer FR. Molecular beacons: probes that fluoresce upon hybridization. Nat Biotechnol 1996; 14: 303-308.

[155] Vet JAM, Van der Rijt BJM and Blom H. Molecular beacons: Colorful analysis of nucleic acids. Expert Rev Mol Diagn 2002; 2: 77-86.

[156] Sando S and Kool ET. Quencher as Leaving Group: Efficient Detection of DNA-Joining Reactions. J Am Chem Soc 2002; 124: 2096-2097.

[157] Powell DH, Ni Dhubhghaill OM, Pubanz D, Helm L, Lebedev YS, Schlaepfer W and Merbach AE. High-pressure NMR kinetics. Part 74. Structural and Dynamic Parameters Obtained from 17O NMR, EPR, and NMRD Studies of Monomeric and Dimeric Gd3+ Complexes of Interest in Magnetic Resonance Imaging: An Integrated and Theoretically Self-Consistent Approach. J Am Chem Soc 1996; 118: 9333-9346.

[158] Caravan P. Strategies for increasing the sensitivity of gadolinium based MRI contrast agents. Chem Soc Rev 2006; 35: 512-523.

[159] Shellock FG and Kanal E. Safety of magnetic resonance imaging contrast agents. J Magn Reson Imaging 1999; 10: 477-484.

[160] Bartolini ME, Pekar J, Chettle DR, McNeill F, Scott A, Sykes J, Prato FS and Moran GR. An investigation of the toxicity of gadolinium based MRI contrast agents using neutron activation analysis. Magn Reson Imaging 2003; 21: 541-544.

[161] Koenig SH and Brown RD, III. Field-cycling relaxometry of protein solutions and tissue: immplications for MRI. Prog Nucl Mag Reson Spectrosc 1990; 22: 487-567.

[162] Ward KM, Aletras AH and Balaban RS. A New Class of Contrast Agents for MRI Based on Proton Chemical Exchange Dependent Saturation Transfer (CEST). J Magn Reson 2000; 143: 79-87.

[163] Zhang S, Winter P, Wu K and Sherry AD. A Novel Europium(III)-Based MRI Contrast Agent. J Am Chem Soc 2001; 123: 1517-1518.

[164] Terreno E, Boniforte P, Botta M, Fedeli F, Milone L, Mortillaro A and Aime S. The water-exchange rate in neutral heptadentate DO3A-like GdIII complexes: Effect of the basicity at the macrocyclic nitrogen site. Eur J Inorg Chem 2003; 11: 3530-3533.

[165] Gunnlaugsson T, Leonard JP, Mulready S and Nieuwenhuyzen M. Three step vs. one pot synthesis and X-ray crystallographic investigation of heptadentate triamide cyclen (1,4,7,10-

tetraazacyclododecane) based ligands and some of their lanthanide ion complexes. Tetrahedron 2004; 60: 105-113.

[166] Woods M, Kovacs Z, Zhang S and Sherry AD. Towards the rational design of magnetic resonance imaging contrast agents: isolation of the two coordination isomers of lanthanide DOTA-type complexes. Angew Chem Int Ed 2003; 42: 5889-5892.

[167] Wu Y, Zhou Y, Ouari O, Woods M, Zhao P, Soesbe TC, Kiefer GE and Sherry AD. Polymeric PARACEST Agents for Enhancing MRI Contrast Sensitivity. J Am Chem Soc 2008; 130: 13854-13855.

[168] Ratnakar SJ, Woods M, Lubag AJM, Kovacs Z and Sherry AD. Modulation of water exchange in europium(III) DOTA-tetraamide complexes via electronic substituent effects. J Am Chem Soc 2008; 130: 6-7.

[169] Zhang S, Trokowski R and Sherry AD. A Paramagnetic CEST Agent for Imaging Glucose by MRI. J Am Chem Soc 2003; 125: 15288-15289.

[170] Kovacs Z and Sherry AD. A general synthesis of 1,7-disubstituted 1,4,7,10-tetraazacyclododecanes. J Chem Soc Chem Commun 1995; 36; 185-186.

[171] Bellouard F, Chuburu F, Kervarec N, Toupet L, Triki S, Le Mest Y and Handel H. cis-Diprotected cyclams and cyclens: a new route to symmetrically or asymmetrically 1,4-disubstituted tetraazamacrocycles and to asymmetrically tetrasubstituted derivatives. J. Chem Soc Perkin Trans 1 1999; 23: 3499-3505.

[172] Trokowski R, Zhang S and Sherry AD. Cyclen-Based Phenylboronate Ligands and Their Eu3+ Complexes for Sensing Glucose by MRI. Bioconjugate Chem 2004; 15: 1431-1440.

[173] Que EL, Gianolio E, Baker SL, Wong AP, Aime S and Chang CJ. Copper-Responsive Magnetic Resonance Imaging Contrast Agents. J Am Chem Soc 2009; 131: 8527-8536.

[174] Chen JW, Pham W, Weissleder R and Bogdanov A, Jr. Human myeloperoxidase: a potential target for molecular MR imaging in atherosclerosis. Magn Reson Med 2004; 52: 1021-1028.

[175] Querol M, Chen JW, Weissleder R and Bogdanov A, Jr. DTPA-bisamide-Based MR Sensor Agents for Peroxidase Imaging. Org Lett 2005; 7: 1719-1722.

[176] Zong Y, Wang X, Jeong E-K, Parker DL and Lu Z-R. Structural effect on degradability and in vivo contrast enhancement of polydisulfide Gd(III) complexes as biodegradable macromolecular MRI contrast agents. Magn Reson Imaging 2009; 27: 503-511.

[177] Douglas T and Young M. Host-guest encapsulation of materials by assembled virus protein cages. Nature (London) 1998; 393: 152-155.

[178] Raja KS, Wang Q, Gonzalez MJ, Manchester M, Johnson JE and Finn MG. Hybrid Virus-Polymer Materials. 1. Synthesis and Properties of PEG-Decorated Cowpea Mosaic Virus. Biomacromolecules 2003; 4: 472-476.

[179] Vasalatiy O, Gerard RD, Zhao P, Sun X and Sherry AD. Labeling of Adenovirus Particles with PARACEST Agents. Bioconjugate Chem 2008; 19: 598-606.

[180] Anderson EA, Isaacman S, Peabody DS, Wang EY, Canary JW and Kirshenbaum K. Viral Nanoparticles Donning a Paramagnetic Coat: Conjugation of MRI Contrast Agents to the MS2 Capsid. Nano Lett 2006; 6: 1160-1164.

[181] Zinn KR, Douglas JT, Smyth CA, Liu HG, Wu Q, Krasnykh VN, Mountz JD, Curiel DT and Mountz JM. Imaging and tissue biodistribution of 99mTc-labeled adenovirus knob (serotype 5). Gene Ther 1998; 5: 798-808.

[182] Botnar RM, Perez AS, Witte S, Wiethoff AJ, Laredo J, Hamilton J, Quist W, Parsons EC, Vaidya A, Kolodziej A, Barrett JA, Graham PB, Weisskoff RM, Manning WJ and Johnstone MT. In Vivo Molecular Imaging of Acute and Subacute Thrombosis Using a Fibrin-Binding Magnetic Resonance Imaging Contrast Agent. Circulation 2004; 109: 2023-2029.

[183] Botnar Rene M, Buecker A, Wiethoff Andrea J, Parsons Edward C Jr, Katoh M, Katsimaglis G, Weisskoff Robert M, Lauffer Randall B, Graham Philip B, Gunther Rolf W, Manning Warren J and Spuentrup E. In vivo magnetic resonance imaging of coronary thrombosis using a fibrin-binding molecular magnetic resonance contrast agent. Circulation 2004; 110: 1463-1466.

[184] Nair SA, Kolodziej AF, Bhole G, Greenfield MT, McMurry TJ and Caravan P. Monovalent and bivalent fibrin-specific MRI contrast agents for detection of thrombus. Angew Chem Int Ed 2008; 47: 4918-4921.

[185] Gao J, Gu H and Xu B. Multifunctional Magnetic Nanoparticles: Design, Synthesis, and Biomedical Applications. Acc Chem Res 2009; 42: 1097-1107.

[186] Cormode DP, Skajaa T, Fayad ZA and Mulder WJM. Nanotechnology in Medical Imaging. Arterioscler Thromb Vasc Biol 2009; 29: 992-1000.

[187] Weissleder R, Kelly K, Sun EY, Shtatland T and Josephson L. Cell-specific targeting of nanoparticles by multivalent attachment of small molecules. Nat Biotechnol 2005; 23: 1418-1423.

[188] Peng X-H, Qian X, Mao H, Wang AY, Chen Z, Nie S and Shin DM. Targeted magnetic iron oxide nanoparticles for tumor imaging and therapy. Int J Nanomed 2008; 3: 311-321.

[189] Zimmer C, Wright SC Jr, Engelhardt RT, Johnson GA, Kramm C, Breakefield XO and Weissleder R. Tumor cell endocytosis imaging facilitates delineation of the glioma-brain interface. Exp Neurol 1997; 143: 61-69.

[190] Medarova Z, Pham W, Farrar C, Petkova V and Moore A. In vivo imaging of siRNA delivery and silencing in tumors. Nat Med 2006; 13: 372-377.

[191] Moore A, Medarova Z, Potthast A and Dai G. In

Vivo Targeting of Underglycosylated MUC-1 Tumor Antigen Using a Multimodal Imaging Probe. Cancer Res 2004; 64: 1821-1827.

[192] Weissleder R, Elizondo G, Wittenberg J, Rabito CA, Bengele HH and Josephson L. Ultrasmall superparamagnetic iron oxide: characterization of a new class of contrast agents for MR imaging. Radiology 1990; 175: 489-493.

[193] Weissleder R, Elizondo G, Wittenberg J, Lee AS, Josephson L and Brady TJ. Ultrasmall superparamagnetic iron oxide: an intravenous contrast agent for assessing lymph nodes with MR imaging. Radiology 1990; 175: 494-498.

[194] Ruehm Stefan G, Corot C, Vogt P, Cristina H and Debatin Jorg F. Ultrasmall superparamagnetic iron oxide-enhanced MR imaging of atherosclerotic plaque in hyperlipidemic rabbits. Acad Radiol 2002; 9 Suppl 1: S143-144.

[195] Tang TY, Howarth SPS, Miller SR, Graves MJ, Patterson AJ, U-King-Im J-M, Li ZY, Walsh SR, Brown AP, Kirkpatrick PJ, Warburton EA, Hayes PD, Varty K, Boyle JR, Gaunt ME, Zalewski A and Gillard JH. The ATHEROMA (atorvastatin therapy: effects on reduction of macrophage activity) study: evaluation using ultrasmall superparamagnetic iron oxide-enhanced magnetic resonance imaging in carotid disease. J Am Coll Cardiol 2009; 53: 2039-2050.

[196] Winter PM, Caruthers SD, Yu X, Song S-K, Chen J, Miller B, Bulte JWM, Robertson JD, Gaffney PJ, Wickline SA and Lanza GM. Improved molecular imaging contrast agent for detection of human thrombus. Magn Reson Med 2003; 50: 411-416.

[197] Winter PM, Cai K, Chen J, Adair CR, Kiefer GE, Athey PS, Gaffney PJ, Buff CE, Robertson JD, Caruthers SD, Wickline SA and Lanza GM. Targeted PARACEST nanoparticle contrast agent for the detection of fibrin. Magn Reson Med 2006; 56: 1384-1388.

[198] Flacke S, Fischer S, Scott MJ, Fuhrhop RJ, Allen JS, McLean M, Winter P, Sicard GA, Gaffney PJ, Wickline SA and Lanza GM. Novel MRI contrast agent for molecular imaging of fibrin. Implications for detecting vulnerable plaques. Circulation 2001; 104: 1280-1285.

[199] Majoros IJ, Thomas TP, Mehta CB and Baker JR, Jr. Poly(amidoamine) dendrimer-based multifunctional engineered nanodevice for cancer therapy. J Med Chem 2005; 48: 5892-5899.

[200] Barrett T, Ravizzini G, Choyke Peter L and Kobayashi H. Dendrimers in medical nanotechnology. IEEE Eng Med Biol Mag 2009; 28: 12-22.